FISEVIER

Contents lists available at ScienceDirect

General and Comparative Endocrinology

journal homepage: www.elsevier.com/locate/ygcen



Hormonal control of the crustacean molting gland: Insights from transcriptomics and proteomics



Donald L. Mykles^{a,b,*}, Ernest S. Chang^b

- ^a Department of Biology, Colorado State University, Fort Collins, CO 80523, USA
- ^b University of California-Davis Bodega Marine Laboratory, Bodega Bay, CA 94923, USA

ARTICLE INFO

Keywords: Y-organ Molting mTOR Ecdysteroid Molt-inhibiting hormone Nitric oxide

ABSTRACT

Endocrine control of molting in decapod crustaceans involves the eyestalk neurosecretory center (X-organ/sinus gland complex), regenerating limbs, and a pair of Y-organs (YOs), as molting is induced by eyestalk ablation or multiple leg autotomy and suspended in early premolt by limb bud autotomy. Molt-inhibiting hormone (MIH) and crustacean hyperglycemic hormone (CHH), produced in the X-organ/sinus gland complex, inhibit the YO. The YO transitions through four physiological states over the molt cycle: basal in intermolt; activated in early premolt; committed in mid- and late premolt; and repressed in postmolt. We assembled the first comprehensive YO transcriptome over the molt cycle in the land crab, Gecarcinus lateralis, showing that as many as 23 signaling pathways may interact in controlling ecdysteroidogenesis. A proposed model of the MIH/cyclic nucleotide pathway, which maintains the basal YO, consists of cAMP/Ca²⁺ triggering and nitric oxide (NO)/cGMP summation phases. Mechanistic target of rapamycin (mTOR) signaling is required for YO activation in early premolt and affects the mRNA levels of thousands of genes. Transforming Growth Factor-β (TGFβ)/Activin signaling is required for YO commitment in mid-premolt and high ecdysteroid titers at the end of premolt may trigger YO repression. The G. lateralis YO expresses 99 G protein-coupled receptors, three of which are putative receptors for MIH/CHH. Proteomic analysis shows the importance of radical oxygen species scavenging, cytoskeleton, vesicular secretion, immune response, and protein homeostasis and turnover proteins associated with YO function over the molt cycle. In addition to eyestalk ganglia, MIH mRNA and protein are present in brain, optic nerve, ventral nerve cord, and thoracic ganglion, suggesting that they are secondary sources of MIH. Down-regulation of mTOR signaling genes, in particular Ras homolog enriched in brain or Rheb, compensates for the effects of elevated temperature in the YO, heart, and eyestalk ganglia in juvenile Metacarcinus magister. Rheb expression increases in the activated and committed YO. These data suggest that mTOR plays a central role in mediating molt regulation by physiological and environmental factors.

1. Introduction

The phenomenon of molting in decapod crustaceans has fascinated biologists for centuries, extending back to the first published descriptions of ecdysis in crayfish by Reamur in 1718 (Reamur, 1718a, b). Advances during the last half of the 20th century established the framework for molecular mechanisms of endocrine control. These studies often used a gene-by-gene approach and relied on RT-PCR cloning of known genes. More recently, high throughput RNA sequencing technology (RNA-seq), in concert with *de novo* assembly and gene annotation tools, ushered in a new era in which it is now possible to obtain sequences of every transcript expressed in a tissue at any moment in any organism (Das and Mykles, 2016; Mykles et al., 2016).

This review emphasizes research published since our 2011 review

(Chang and Mykles, 2011). The reader is referred to previous review articles, cited in Chang and Mykles (2011) and Covi et al. (2009, 2012), which cover the earlier research in greater depth. Advances in transcriptomics and proteomics have given us new insights into the phenotypic plasticity of the Y-organ (YO), as well as served as tools of discovery of signaling pathways that integrate physiological and environmental factors that control YO ecdysteroidogenesis.

2. Overview of crustacean molting and its control

Ecdysis or exuviation, the active shedding of the exoskeleton, marks a pivotal event in organismal growth of crustaceans and other arthropods. Molting, as defined here, encompasses the preparatory events leading to ecdysis, ecdysis, and the events following ecdysis. These

^{*} Corresponding author.

Table 1General schedule of molt cycle events in decapod crustaceans. Modified from Skinner (1962). R index applies to *G. lateralis* (Yu et al., 2002).

Molt Stage	Event		
Ecdysis (E)	Low hemolymph ecdysteroid titers.		
	Active shedding of old exoskeleton.		
Metecdysis (Postmolt)			
A	Low hemolymph ecdysteroid titers.		
	Continued swallowing of water or air expands new		
	exoskeleton and extends regenerated limbs.		
В	Low hemolymph ecdysteroid titers.		
	Endocuticle synthesis begins.		
$C_1, C_2, \& C_3$	Low hemolymph ecdysteroid titers.		
	Endocuticle synthesis and calcification.		
	Membranous layer forms in C_3 .		
Anecdysis (Intermolt)			
C_4	Low hemolymph ecdysteroid titers.		
	Exoskeleton fully formed and calcified.		
	Tissue growth & storage of organic reserves in		
	hepatopancreas.		
	Formation of basal regenerates at autotomized limbs $(R = 8-10)$		
Proecdysis (Premolt)	(10 0 10)		
D ₀ (early premolt)	Hemolymph ecdysteroid titers increase.		
D ₀ (carry premote)	Calcium storage in gastroliths or concretions in		
	hepatopancreas.		
	Claw muscle atrophy.		
	Growth of primary limb regenerates ($R = 12-16$).		
	Regeneration and growth of autotomized limbs or		
	secondary limb regenerates.		
D ₁ (mid premolt)	Hemolymph ecdysteroid titers increase further.		
	Separation of epidermis from exoskeleton (apolysis).		
	Degradation of old exoskeleton, starting with membranous		
	layer.		
	Claw muscle atrophy continues.		
	Growth of limb regenerates ($R = 16-24$).		
D ₂₋₃ (late premolt)	Hemolymph ecdysteroid titers increase rapidly; reach peak		
	in D ₃ .		
	Epicuticle and exocuticle synthesized.		
	Limb regenerates fully grown (R = \sim 24).		
	Hemolymph ecdysteroid titers reach peak in D ₃ , then		
D	decrease.		
D_4	Hemolymph pink from astaxanthin resorbed from		
	exocuticle.		
	Swallowing of water or air initiated.		

events, which are initiated and coordinated by ecdysteroids synthesized by the YO, define the stages of the molt cycle (Table 1). The molt cycle is divided into four major stages: anecdysis (intermolt or stage C₄), proecdysis (premolt or stage D), ecdysis (E), and metecdysis (postmolt) (Drach, 1939; Spindler et al., 1974). Premolt is further divided into early (stage D₀), mid (stage D₁), and late (stages D₂, D₃, and D₄) substages. Postmolt is further divided into A_{1-2} , B_{1-2} , and C_{1-3} substages (Drach and Tchernigovtzeff, 1967; Skinner, 1962). During premolt, the outer two layers (epicuticle and exocuticle) of the new exoskeleton are synthesized, the inner layers (membranous layer and endocuticle) of the old exoskeleton are degraded, calcium is resorbed from the old exoskeleton and stored in gastroliths and/or as concretions in the hepatopancreas, the claw closer muscle atrophies, and regenerates of autotomized appendages grow (Hopkins and Das, 2015; McCarthy and Skinner, 1977; Mykles, 2001; Skinner, 1985). The reduced size of the closer muscle facilitates withdrawal of the claws at ecdysis (Mykles and Medler, 2015). Ecdysis, which is triggered by a rapid drop in hemolymph ecdysteroid titers at the end of premolt, begins with the swallowing of water in aquatic species or air in terrestrial species to expand the stomach and lift the carapace (Cheng and Chang, 1991; Mykles, 1980, 2011; Skinner, 1985). Immediately after ecdysis, the internal hydrostatic pressure from continued water or air swallowing expands the new exoskeleton and supports movement until the exoskeleton is sufficiently hardened (Mykles, 1980; Taylor and Kier, 2003, 2006). In aquatic marine species, such as American lobster (Homarus americanus),

hemolymph volume expands from the isosmotic transport of water by the intestine (Mykles, 1980). For terrestrial species, such as the blackback land crab, *Gecarcinus lateralis*, hemolymph volume expansion results from imbibing water, diet, and/or water uptake from the substrate via the gills (Bliss, 1979). Hemolymph ecdysteroid levels are lowest during postmolt (Mykles, 2011). The combination of hemolymph ecdysteroid titer, limb bud size as expressed by the regeneration (R) index, and the structure of the exoskeleton and underlying epithelium are used to determine the molt stage (Table 1) (Covi et al., 2010; Mykles, 2011; Skinner, 1962; Snyder and Chang, 1991; Yu et al., 2002).

Molting is induced in many decapods by multiple leg autotomy (MLA) or by eyestalk ablation (ESA). Both methods have been used for decades to stimulate precocious molts in intermolt animals (Smith. 1940; Zeleny, 1905). ESA removes the primary source of molt-inhibiting hormone (MIH), resulting in immediate YO activation and entry into premolt by one day post-ESA (Chang and Bruce, 1980; Chang and Mykles, 2011; Covi et al., 2010). In G. lateralis, adult animals reach ecdysis about three weeks post-ESA, but usually fail to exuviate successfully (Covi et al., 2010). By contrast, eyestalk-ablated juvenile H. americanus and young crayfish successfully molt and show shortened molt intervals over multiple molt cycles, resulting in accelerated growth (Chang, 1985, 1989; Smith, 1940). Decapods can regenerate appendages lost to predation or injury, but they must molt to regain functional limbs (Hopkins and Das, 2015). However, molting is induced only with the loss of a sufficient number of appendages that impairs mobility. This is particularly crucial for species living in terrestrial habitats, which lack the neutral buoyancy of water to support the body. In G. lateralis, autotomy of at least five walking legs stimulates molting (Skinner and Graham, 1970, 1972). A basal regenerate forms at the autotomy plane and remains small until the animal enters premolt, when increasing ecdysteroid titers stimulate limb bud growth (Hopkins and Das. 2015). Animals usually enter premolt four to six weeks after MLA and molt about three weeks later (Covi et al., 2010; Yu et al., 2002). In G. lateralis, limb bud autotomy (LBA) in early premolt suspends molting processes two to three weeks by lowering hemolymph ecdysteroid titers (Yu et al., 2002). This allows sufficient time for a secondary regenerate to differentiate and grow, so that individuals molt with a full complement of walking legs (Holland and Skinner, 1976; Mykles, 2001; Yu et al., 2002).

The YOs synthesize hydroxylated steroid hormones (ecdysteroids) (Mykles, 2011). The YOs are negatively regulated by the inhibitory neuropeptides MIH and crustacean hyperglycemic hormone (CHH), which are synthesized in the X-organ/sinus gland complex in the eyestalk ganglia (Hopkins, 2012; Webster, 2015a, 2015b; Webster et al., 2012). The YO converts cholesterol obtained from the diet to 25deoxyecdysone (25dE) and ecdysone, depending on species, by stage 1 (e.g., Neverland, Nvd and Spook, Spo) and stage 2 (Halloween genes Phantom, Phm; Disembodied, Dib; and Shadow, Sad) enzymes (Table 2) (Mykles, 2011; Niwa and Niwa, 2014). A 20-hydroxyecdysone (20E) hydroxylase, designated Shade in insects and Shed in decapods, converts 25dE and ecdysone to the active molting hormones ponasterone A and 20E, respectively (Mykles, 2011; Ventura et al., 2017, 2018). The G. lateralis YO expresses six Shed P450 orthologs, suggesting that the YO can secrete 20E (Swall et al., 2019). The activity of transaldolase, a pentose phosphate pathway enzyme that generates NADPH, is correlated with YO ecdysteroid synthesis and is inhibited by MIH (Lachaise et al., 1996). As many of the ecdysteroidogenic enzymes require NADPH, inhibition of transaldolase would be an effective mechanism for post-translational control of ecdysteroid biosynthesis. All these genes are expressed in the YO (Table 2) (Das et al., 2016; Shyamal et al., 2018; Sin et al., 2014; Tom et al., 2013). The YO also expresses ecdysteroid receptor and ecdysteroid-responsive genes (Table 2), suggesting that the YO is autoregulated by ecdysteroids.

The YO transitions through four distinct physiological states over the molt cycle; these are the basal, activated, committed, and repressed phenotypes (Fig. 1). During intermolt, the pulsatile release of MIH

Table 2 Selected signaling genes identified in the *G. lateralis* YO transcriptome (Das et al., 2016, 2018; Shyamal et al., 2018).

Pathway	Genes (Abbreviations)		
MIH	Adenylyl cyclases (Adcy1, 2, 9), protein kinases A & G (PKA, PKG), calmodulin (CALM), calcineurin (CALN), NO synthase (NOS), NO-		
mTOR	sensitive guanylyl cyclase (GC-I), cyclic nucleotide phosphodiesterases (PDEs 1, 2, 3, 4, 5, 7, 9, & 11) mTOR, tuberous sclerosis complex (TSC), Raptor, mLST8, Rheb, Pl3 kinase, phosphoinositide-dependent kinase 1 (PDK1), protein kinase B (Akt), ribosome subunit 6 kinase (S6K), 4E-binding protein-1 (4E-BP1), FK506-binding protein-12 (FKBP12), hypoxia inducible factor 1 (HIF1), AMP kinase (AMPK)		
тдгр	Myostatin-like (Mstn), activin receptor subunit I (ACVR-I), R-Smads (Smad1, Smad2/3), Co-Smad (Smad4), I-Smad (Smad6), protein phosphatase 2 (PP2), bone morphogenic protein (BMP), BMP and activin membrane-bound inhibitor homolog (BAMBI), follistatin		
Mitogen-activated protein (MAP) kinase	Growth factor receptor-bound protein (GRB), MAP kinase kinase (MEK1), MAP kinase (ERK), MAPK-activated protein kinase (MNK1/2), cAMP response element-binding protein (CREB), c-Myc, serum response factor (SRF), Ras		
Hedgehog	Patched (Ptc), Smoothened (Smo), Fused (Fu), Cubitus interruptus (Ci), γ-secretase		
Notch	Notch, Fringe, Delta, Dishevelled (Dsh/Dvl)		
Wnt (wingless/int)	Wnt, Adenomatous polyposis coli (APC), β-catenin, Axin		
Ecdysteroid	Ecdysteroid receptor (EcR, RXR), ecdysteroid response genes [E74, E75, HR3, HR4, Broad Complex (BrC), fushi tarazu-F1 (βFtz-F1)], ecdysteroid biosynthesis [Transaldolase (Taldo), Neverland (Nvd), Spook (Spo), Phantom (Phm), Disembodied (Dib), Shadow (Sad), Shed]		

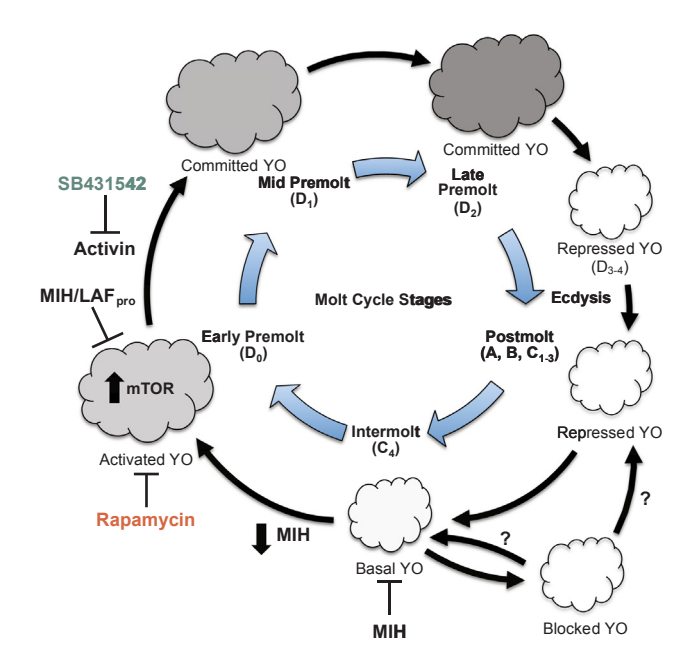


Fig. 1. YO regulation over the molt cycle in G. lateralis. The YO transitions through basal, activated, committed, and repressed phenotypes at intermolt (stage C_4), early premolt (stage D_0), mid/late premolt (stages D_1 and D_2), and postmolt (stages A, B, and C₁₋₃), respectively. During intermolt, MIH release from the eyestalk X-organ/sinus gland complex maintains the YO in the basal state. Reduced MIH release activates the YO via mTOR, which is inhibited by rapamycin. TGFβ/Activin signaling, which is inhibited by SB431542, mediates YO transition from the activated to committed phenotype. Elevated ecdysteroid titers at the end of premolt are hypothesized to drive the transition to the repressed phenotype. Some animals enter a blocked state, in which animals are refractory to molt induction by multiple leg autotomy. Basal and activated YOs are sensitive to MIH, CHH, and limb autotomy factor - proecdysis (LAF_{pro}), which is secreted by limb regenerates; committed and repressed YOs are refractory to MIH, CHH, and $LAF_{\rm pro}$. Size indicates YO hypertrophy and shading indicates relative ecdysteroidogenic activity (lowest in postmolt; highest in D2). Modified from Das and Mykles (2016).

maintains the YO in the basal state. The basal YO secretes ecdysteroids at low rates, maintaining low hemolymph ecdysteroid titers (Mykles, 2011). A reduction in MIH release initiates YO activation in early premolt (stage D_0). YO activation requires mechanistic target of rapamycin (mTOR) activity (Abuhagr et al., 2014b, 2016). The YO hypertrophies to increase ecdysteroid synthetic capacity, while remaining sensitive to MIH (Devi et al., 2015; Lachaise et al., 1993; Shyamal et al., 2014; Smija and Sudha, 2016). The activated YO is also sensitive to limb autotomy factor - proecdysis (LAF $_{\rm pro}$), which is produced by

secondary limb buds following LBA (Mykles, 2001; Skinner, 1985; Yu et al., 2002). A critical decision point occurs at the end of early premolt (stage D_0), when animals become committed to molt; the YO transitions to the committed phenotype in mid- and late premolt (Fig. 1). This transition is mediated by transforming growth factor beta (TGF β)/Activin (Abuhagr et al., 2016). The committed YO is insensitive to MIH and other inhibitory neuropeptides and has maximum ecdysteroidogenic activity (Chang and Mykles, 2011). At the end of late premolt, the YO transitions to the repressed phenotype, which is characterized by very low ecdysteroidogenic activity (Fig. 1). We hypothesize that the peak in hemolymph titer prior to ecdysis triggers the committed to repressed transition (Chang and Mykles, 2011; Dell et al., 1999). The YO remains in the repressed state through postmolt and returns to the basal state by intermolt (Fig. 1).

In some decapod species, adults enter terminal anecdysis and no longer molt. Adult green shore crab, Carcinus maenas, are refractory to ESA and MLA (Abuhagr et al., 2014a; McDonald et al., 2011). In some G. lateralis individuals, MLA does not induce molting; these "blocked" animals fail to enter premolt by 12 weeks post-MLA and are refractory to ESA (Pitts et al., 2017). A qPCR analysis suggests that the eyestalk ganglia/YO endocrine axis is chronically inhibited in blocked animals through increased expression of neuropeptide and mTOR signaling genes in the eyestalk ganglia and neuropeptide signaling genes in the YO. Six of seven neuropeptide signaling genes (Gl-MIH; Gl-CHH; Gl-Nitric oxide synthase, Gl-NOS; Gl-Guanylyl cyclase-IB, Gl-GC-IB; Gl-GC-II; and Gl-GC-III) are up-regulated between 82- and 390-fold and three of four mTOR signaling genes (Gl-mTOR; Gl-Rheb; and Gl-S6 kinase, Gl-S6K) and Gl-elongation factor 2 (EF2) are up-regulated between 220and 370-fold in the eyestalk ganglia (Pitts et al., 2017). The differences in mRNA levels of neuropeptide signaling genes in the YO are even greater between control and blocked animals. Six of 13 neuropeptide signaling genes (Gl-Adenylyl cyclase, Gl-AC; Gl-Protein kinase A, Gl-PKA; Gl-NOS; Gl-GC-IB; and Gl-Protein kinase G, Gl-PKG) are up-regulated three to four orders of magnitude in the blocked YO (Pitts et al., 2017). In addition, Gl-EF2 level is 250-fold higher in the blocked YO (Pitts et al., 2017). By contrast, there are no differences in mRNA levels of mTOR signaling genes (Gl-mTOR; Gl-Rheb; Gl-Akt; and Gl-S6K), indicating that the blocked YO is not activated. Increased Gl-MIH and Gl-CHH mRNA levels in brain and thoracic ganglion may also contribute to the blocked state as secondary sources of these inhibitory neuropeptides (Pitts and Mykles, 2017; Pitts et al., 2017). These results indicate that the blocked YO constitutes a fifth phenotype that may be associated with terminal anecdysis in some species (Fig. 1).

3. Signaling pathways controlling phase transitions in the Y-organ

3.1. Neuropeptide signaling

Molting in decapod crustaceans is regulated by inhibitory neuropeptides that prevent activation of the YO. MIH is considered the main neuropeptide that controls molting (Chang and Mykles, 2011; Webster et al., 2012). The primary source of MIH is the X-organ/sinus complex in the eyestalk ganglia, but MIH mRNA and peptide are expressed at lower levels in other regions of the central nervous system, such as brain, optic nerve, ventral nerve cord, and thoracic ganglion (Pitts and Mykles, 2017; Stewart et al., 2013). Adults usually molt no more than once per year, which means that MIH must be constitutively secreted for months or years to maintain the intermolt state. What is remarkable is that very little MIH is apparently needed to inhibit the YO. Average concentrations of MIH in the hemolymph are below 5 fmol/ml (5 \times 10 12 M) in intermolt animals, which is too low to inhibit YO ecdysteroidogenesis (Chung and Webster, 2005; Nakatsuji and Sonobe, 2003, 2004; Saïdi et al., 1994; Webster, 1993). However, pulsatile release at roughly 10-minute intervals results in a transient increase in MIH, which quickly decreases with a half-life of ~ 5 min (Chung and Webster, 2005).

It is generally accepted that MIH signaling is mediated by the cyclic nucleotide second messengers cAMP and cGMP (Chang and Mykles, 2011; Covi et al., 2009, 2012). As cAMP and cGMP turnover is very high in the cell, how is YO inhibition sustained between MIH pulses? In 2004, we were the first to characterize a cDNA encoding a calmodulin (CaM)-dependent nitric oxide synthase (NOS) from a crustacean and proposed a mechanistic model that arranged cAMP/Ca²⁺- and NO/cGMP-dependent cassettes in series (Kim et al., 2004a). Subsequently, the model was revised in 2011/2012 to include a putative MIH G protein-coupled receptor (GPCR) and direct inhibition of ecdysteroidogenesis by chronic activation of PKA (Chang and Mykles, 2011; Covi et al., 2012).

The MIH signaling pathway model is presented in Fig. 2. MIH signaling is organized into a cAMP/Ca²⁺-dependent triggering phase, which leads to prolonged activation of a NO/cGMP-dependent summation phase. MIH binds to high-affinity receptors in the YO membrane (Chung and Webster, 2003; Webster, 1993). The MIH GPCR activates adenylyl cyclase (AC), which converts ATP to cAMP. cAMP-dependent protein kinase (PKA) phosphorylates a Ca²⁺ channel, leading to an increase in intracellular Ca²⁺. CaM is a Ca²⁺-binding protein that allosterically activates NOS and calcineurin (CaN), a CaM-dependent protein phosphatase. Phosphorylation by a variety of protein kinases inactivates NOS (Ghimire et al., 2017). Thus, NOS is activated by a combination of dephosphorylation by CaN and direct binding of CaM to the CaM-binding domain in NOS (Fig. 2). NOS converts arginine to citrulline and NO, activating a NO-dependent guanylyl cyclase (GC-I) that converts GTP to cGMP. A constitutively active NO-independent guanylyl cyclase (GC-III) may also play a role (Lee et al., 2007a, b). A cGMP-dependent protein kinase (PKG) inhibits ecdysteroid synthesis, presumably by inhibiting, either directly or indirectly, mTOR activity. The protein substrates of PKG have not been identified.

Cyclic nucleotide phosphodiesterases (PDEs) convert cAMP and cGMP to AMP and GMP, respectively, to reverse the actions of neuropeptides. Eleven PDE families have been identified in mammalian tissues that differ in substrate specificity, modes of regulation, inhibitor sensitivity, and tissue distribution (Francis et al., 2011; Peng et al., 2018). Contigs encoding nine PDE families were identified in the *G. lateralis* YO transcriptome: PDE1, 2, 3, 4, 5, 7, 8, 9, and 11 (Rifai and Mykles, 2019). Pharmacological reagents that are selective for PDE1 and PDE5 inhibit PDE activity in crayfish YO extracts, while inhibitors of PDE2 and PDE4 have no effect (Nakatsuji et al., 2006). PDE1 is a Ca²⁺/CaM-dependent PDE that hydrolyzes both cAMP and cGMP, while PDE5 is a cGMP-specific PDE (Fig. 2) (Francis et al., 2011; Peng et al., 2018). PDEs are hypothesized to have two functions in the YO:

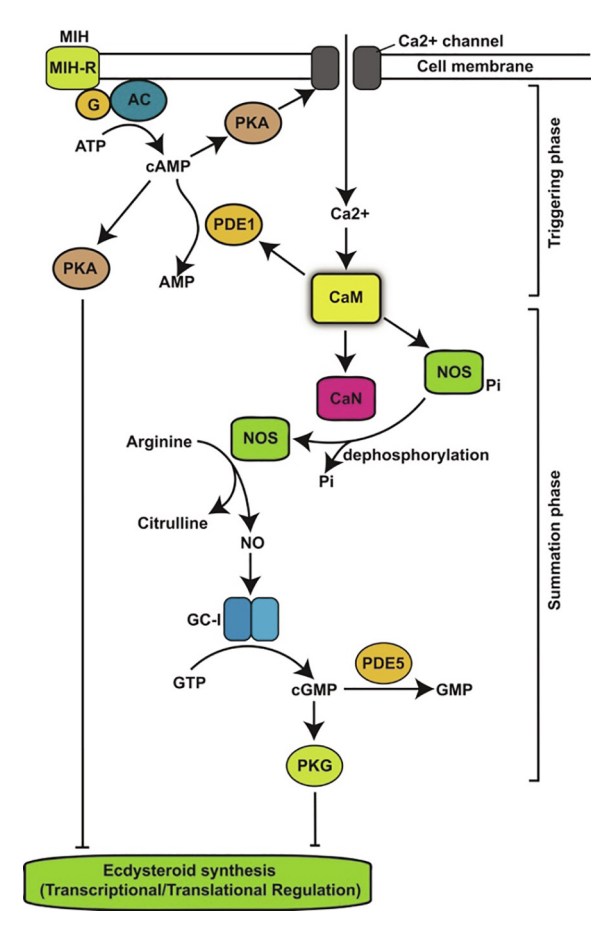


Fig. 2. Proposed model for MIH signaling in the decapod Y-organ. The triggering phase is initiated by binding of MIH to a G protein-coupled receptor (MIH-R) and activation of adenylyl cyclase (AC); cAMP increases intracellular Ca²⁺ via cAMP-dependent protein kinase (PKA) phosphorylation of Ca²⁺ channels. Sensitivity to MIH is determined by phosphodiesterase 1 (PDE1) activity, which varies over the molt cycle. The summation phase is mediated by NO and cGMP. Calmodulin (CaM) links the two phases by activating NO synthase (NOS) directly and indirectly via calcineurin (CaN). Dephosphorylation of NOS by CaN can potentially prolong the response to MIH. CaM can also activate PDE1 to inhibit the triggering phase (PDE1 can also hydrolyze cGMP, thus inhibiting the summation phase). cGMP-dependent protein kinase (PKG) inhibits ecdysteroidogenesis. Chronic activation of PKA may directly inhibit ecdysteroidogenesis. Our assumption is that YOs from all decapods are regulated by the same pathway, but may differ in the sensitivity of the triggering and summation phases. Other abbreviations: G, G protein; GC-I, NO-sensitive guanylyl cyclase; PDE5, cGMP PDE. From Covi et al. (2012).

(1) YO activation in response to reduced MIH release from the sinus gland and (2) modulating the sensitivity of the YO to neuropeptides over the molt cycle. Reduced secretion of MIH from the sinus gland decreases production of cAMP and cGMP; the remaining cyclic nucleotides are inactivated by PDEs (Fig. 2). Consequently, suppression of ecdysteroid synthesis and secretion by PKG is relieved, leading to the activation of the YO. PDEs also play a role in determining the sensitivity of the YO to neuropeptide, as an increase in PDE activity is correlated with reduced sensitivity to MIH and CHH during mid and late premolt (Alexander et al., 2018; Nakatsuji and Sonobe, 2004; Nakatsuji et al., 2006).

The model is supported by experimental studies (see Covi et al., 2012; Nakatsuji et al., 2009 for references to earlier work). First, all the MIH signaling components are expressed in the YO (Table 2) (Das et al., 2016, 2018; Kim et al., 2004a; Lee et al., 2007a, b; Lee and Mykles, 2006; McDonald et al., 2011; Rifai and Mykles, 2019; Shyamal et al., 2018; Tran et al., 2019). Second, ecdysteroid secretion by the YO in

vitro is inhibited by NO donors and by slowly hydrolyzable or non-hydrolyzable analogs of cAMP and cGMP in most species (Covi et al., 2008a, 2009; Mykles et al., 2010a; Nakatsuji et al., 2006). Third, MIH usually causes a small, transient increase in cAMP, followed by a larger, sustained increase in cGMP (Saïdi et al., 1994; Sedlmeier and Fenrich, 1993); see Covi et al., 2009 for additional references}. Fourth, IBMX, a broad spectrum PDE inhibitor, enhances the inhibition of YO ecdysteroidogenesis by MIH in vitro (Nakatsuji et al., 2006). Fifth, forskolin, an activator of adenylyl cyclase, inhibits YO ecdysteroid secretion (Covi et al., 2009). Sixth, NOS and cGMP are localized in the YO (Kim et al., 2004a; McDonald et al., 2011). Seventh, NOS is phosphorylated when the YO is activated by ESA, which indicates that NOS is inactive (Lee and Mykles, 2006). Eighth, YC-1, an activator of GC-I, in combination with IBMX, inhibits YO ecdysteroid secretion in vitro (Covi et al., 2008a; Mykles et al., 2010a). Ninth, ESA increases NOS, GC-I, and GC-III mRNA levels, apparently as a compensatory response to the acute withdrawal of eyestalk neuropeptides; ESA has no effect on membrane guanylyl cyclase (GC-II) mRNA level (Lee et al., 2007a; McDonald et al., 2011).

3.2. mTOR signaling

mTOR is a highly conserved serine/threonine protein kinase belonging to the PI3 kinase-related kinase family that mediates the allocation of cellular energy and resources in response to nutrients, growth factors, and stress in animal and plant cells (Cao et al., 2019; Kim and Guan, 2019; Liu and Sabatini, 2019; Saxton and Sabatini, 2017; Shi et al., 2018; Weichhart, 2018). mTOR associates with Raptor, mLST8, and other proteins to form the mTOR complex 1 (mTORC1), which supports global protein synthesis by stimulating mRNA translation and ribosome biogenesis (Cao et al., 2019; Kim and Guan, 2019; Liu and Sabatini, 2019). Two primary targets of mTORC1 are ribosomal protein S6 kinase (S6K) and eukaryotic Initiation Factor (eIF) 4E-binding protein (4EBP). Phosphorvlated 4EBP releases eIF4E, which is required for 5' cap-dependent translation (Liu and Sabatini, 2019). Both S6K and mTORC1 activity increase transcription of rRNA to support synthesis of new ribosomes (Liu and Sabatini, 2019). Thus, phosphorylation of S6K and 4EBP by mTORC1 leads to enhanced mRNA and rRNA transcription providing the proteins and ribosomes necessary for cell growth. Rapamycin inhibits mTORC1 through FK506 binding protein 12 (FKBP12) (Hausch et al., 2013). mTORC2, in which Raptor is replaced by Rictor, is involved in actin cytoskeleton organization and apoptosis and is insensitive to rapamycin (Cao et al., 2019; Liu and Sabatini, 2019; Saxton and Sabatini, 2017). There is considerable crosstalk between mTORC1 and mTORC2 that integrate insulin/insulin-like growth factor (IGF) and growth factor/MAP kinase signaling (Liu and Sabatini, 2019).

A key upstream regulator of mTORC1 is the Ras homolog enriched in brain (Rheb) G protein. Rheb-GTP binds to the kinase domain to activate mTORC1 (Groenewoud and Zwartkruis, 2013). Rheb is inhibited by the tuberous sclerosis complex (TSC1/2), a GTPase-activating protein that converts active Rheb-GTP to inactive Rheb-GDP (Liu and Sabatini, 2019). Various signaling pathways converge on TCS1/2 to regulate its activity by phosphorylation. Signaling pathways that stimulate cellular growth, such as growth factor/MAP kinase, insulin/PI3 kinase/Akt, and tumor necrosis factor pathways, inhibit TSC1/2, whereas pathways that inhibit cellular growth, such as AMP kinase (energetic stress), REDD1 (hypoxic stress), and Wnt/GSK3ß stimulate TSC1/2 (Liu and Sabatini, 2019; Saxton and Sabatini, 2017). Transcriptional regulation of Rheb protein levels can also affect mTORC1 activity (Layalle et al., 2008; Romero-Pozuelo et al., 2017; Teleman, 2010; Yang et al., 2006). Thus, Rheb is regulated post-translationally by TSC1/2 and transcriptionally to mediate short-term and long-term effects, respectively, on mTORC1-dependent protein synthesis.

mTORC1 plays a key role in regulating YO ecdysteroidogenesis. MLA and ESA increase expression of mTOR signaling genes in the *G. lateralis* YO and rapamycin blocks the ESA-induced increases in mTOR

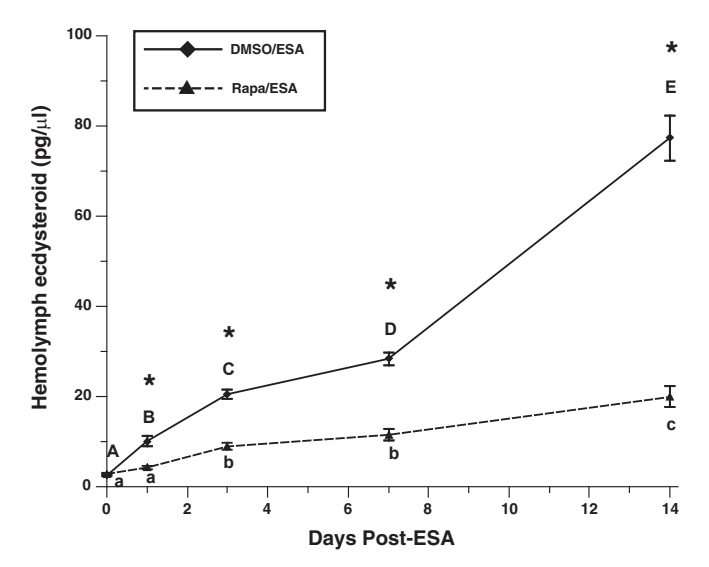


Fig. 3. Effect of mTOR inhibitor rapamycin on hemolymph ecdysteroid titers in *G. lateralis in vivo*. Animals were eyestalk-ablated at Day 0 and injected with a single dose of rapamycin (\sim 10 μ M final hemolymph concentration) or equal volume of DMSO (\sim 0.1% final hemolymph volume). Data presented as mean \pm 1 s.e.m. (n = 5–8). Asterisks indicate means that were significantly different (P < 0.05) between control and rapamycin at the same time point. Letters indicate significant differences in the means within a treatment (upper case for control; lower case for rapamycin); means that were not significantly different share the same letter. From Abuhagr et al. (2016).

signaling gene expression (Abuhagr et al., 2014b, 2016; Das et al., 2018; Shyamal et al., 2018). In particular, increased Rheb mRNA levels are correlated with increased ecdysteroidogenesis during premolt in G. lateralis and Metacarcinus magister (Abuhagr et al., 2016; Das et al., 2018; Shyamal et al., 2018; Wittmann et al., 2018). Increased Gl-Rheb mRNA level is correlated with increased protein synthesis in the claw muscle of premolt G. lateralis (MacLea et al., 2012; Mykles and Medler, 2015). Acclimation of juvenile M. magister to increasing temperatures decreases the Mm-Rheb mRNA levels in YO, eyestalk ganglia, and heart as a compensatory response to increased metabolic rates (Wittmann et al., 2018). By contrast, in a limited study of the C. maenas YO, molt stage has no effect on mTOR signaling genes (Cm-mTOR, Cm-Rheb, Cm-Akt, and Cm-S6K) (Abuhagr et al., 2014b). In in vitro studies, rapamycin at concentrations as low as 0.2 µM inhibit YO ecdysteroid secretion in C. maenas and G. lateralis (Abuhagr et al., 2014b). Rapamycin blocks the ESA-induced increase in hemolymph ecdysteroid titers in G. lateralis, indicating that mTORC1 activity is required for YO activation and entry into premolt (Fig. 3). These data indicate that mTORC1-dependent protein synthesis is required for molting gland activation in crustaceans. Moreover, Rheb expression can be used as an indicator of the effects of temperature and perhaps other stressors on mTORC1 activity.

3.3. TGFβ/Activin signaling

TGF β proteins act as autocrine factors. In other words, their action is highly localized and largely affects the same tissue in which they are synthesized. It is secreted as an inactive complex consisting of the inhibitory propeptide bound to mature peptide dimer; proteolytic cleavage of the propeptide releases the mature peptide, which binds to cell surface receptors (Derynck and Budi, 2019). Members of the TGF β superfamily include TGF β isoforms, bone morphogenetic proteins (BMPs), growth differentiation factors (GDFs), Activins, Inhibins, Nodals, and Müllerian inhibitory factor (Nickel et al., 2018). These ligands bind to distinct receptors, which activate Smad transcription factors that regulate gene expression through transcriptional activation or repression (Budi et al., 2017; Derynck and Budi, 2019; Luo, 2017; Macias et al.,

2015). In the canonical pathway (Derynck and Budi, 2019; Macias et al., 2015), signaling is initiated when a ligand forms a complex with Type I and II receptors, which phosphorylate R-Smad. Two phosphorylated R-Smad monomers form a trimeric complex with one Co-Smad in the cytosol. The R-Smad/Co-Smad trimer translocates to the nucleus, binds to promoter regions, and recruits transcriptional coregulators to effect gene transcription (Derynck and Budi, 2019). Inhibitory (I)-Smads can bind to Type I receptors to block R-Smad phosphorylation (Derynck and Budi, 2019). There is extensive crosstalk with other signaling pathways (e.g., MAPK, Wnt, PI3K-Akt, JAK, Hedgehog, and Notch) that modulate TGFβ/Smad signaling (Derynck and Budi, 2019).

A myostatin (Mstn)-like factor mediates the transition of the YO from the activated to the committed state during premolt. An invertebrate Mstn-like transcript was first identified in bay scallop muscle and was subsequently characterized in G. lateralis muscle (Covi et al., 2008b; Kim et al., 2004b). Mstn has now been identified in many decapod species and is expressed in a wide variety of tissues, with generally higher mRNA levels in YO, muscle, and heart (Abuhagr et al., 2016; Covi et al., 2010, 2008b; Das et al., 2018; De Santis et al., 2011; Kim et al., 2009, 2010; Lee et al., 2015; Lv et al., 2014; MacLea et al., 2010; Qian et al., 2013; Sarasvathi et al., 2015; Shen et al., 2015; Shyamal et al., 2018; Ventura et al., 2014; Zhuo et al., 2017). The Mstn-like protein has signal peptide, propeptide, and mature peptide regions characteristic of the TGF\$\beta\$ superfamily and clusters in the Mstn/Activin/GDF-11 clade (Covi et al., 2008b; De Santis et al., 2011; Qian et al., 2013; Shen et al., 2015; Zhou et al., 2019; Zhuo et al., 2017). In G. lateralis, conserved proteolytic cleavage sites between the signal peptide and propeptide sequences and between the propeptide and mature peptide sequences are predicted to produce a 363-amino acid propeptide and a 110-amino acid mature peptide, respectively (Covi et al., 2008b). The mature peptide has nine conserved cysteines that form four intrachain disulfide bonds and one interchain disulfide bond to stabilize the homodimeric structure of the secreted protein (Covi et al., 2008b; De Santis et al., 2011; Qian et al., 2013; Sarasvathi et al., 2015; Shen et al., 2015; Zhuo et al., 2017). Decapod tissues express Mstn variants that are generated by alternative splicing (Covi et al., 2008b; Zhuo et al., 2017). The functions of these splice variants are

SB431542, a highly specific inhibitor of the Activin RI receptor, blocks Activin signal transduction, but has no effect on other TGF β signaling pathways, including BMP (Inman et al., 2002). When injected into eyestalk-ablated *G. lateralis* at Day 0, SB431542 (10 μ M estimated concentration in the hemolymph) decreases hemolymph ecdysteroid titers by 7 days post-ESA to a titer similar to that at 1 day post-ESA (Fig. 4A) and blocks the ESA-induced increases in mTOR signaling gene mRNA levels (Fig. 4B-F) (Abuhagr et al., 2016). The Day 7 time point is especially significant, as this is when ESA animals transition from early premolt (stage D₀) to mid-premolt (stage D₁) and become committed to molt (Covi et al., 2010). Activin/Smad signaling is not necessary for activation, as the increased ecdysteroid titers and mTOR signaling gene expression in ESA animals \pm SB431542 are the same at days 1 and 3 post-ESA (Fig. 4A) (Abuhagr et al., 2016). These data indicate that Activin/Smad signaling mediates YO transition to the committed state.

4. Transcriptomic analysis of the Y-organ

Transcriptomic analysis of the YO from *G. lateralis* and crayfish, *Pontastacus leptodactylus*, reveals complex expression profiles of thousands of genes. As expected, the YO expresses the genes in the ecdysteroid biosynthetic pathway (Table 2) (Shyamal et al., 2018; Tom et al., 2013). Deep high throughput RNA sequencing (RNA-seq) of the YO from intermolt *G. lateralis* yielded a comprehensive catalog of contiguous sequences (contigs) (Das et al., 2016). This baseline transcriptome of 288,673 contigs was *de novo* assembled from nearly 228 million reads (Das et al., 2016). The crayfish YO transcriptome is not as

extensive (74,877 contigs), but the gene expression profiles are similar between the two species (Das et al., 2016; Tom et al., 2013). Both transcriptomes express a large diversity of signaling pathway genes (Das et al., 2016). These include MIH, mTOR, $TGF\beta$, MAPK, Hedgehog, Notch, Wnt, and ecdysteroid signaling (Tables 2, 3) (Das et al., 2016, 2018; Shyamal et al., 2018).

4.1. Analysis of the YO over the molt cycle

A YO transcriptome was assembled from 15 cDNA libraries representing five molt stages (intermolt, IM; early premolt, EP; mid-premolt, MP; late premolt, LP; and postmolt, PM) from G. lateralis induced to molt by MLA (Das et al., 2018). The reference transcriptome of 229,780 contigs was assembled from \sim 568 million paired and unpaired reads (Das et al., 2018). Elimination of viral sequences, prokaryotic sequences, three outlier sequences of > 2 million counts, and low-abundant sequences produced a filtered transcriptome of 48,590 contigs used for annotation and differential gene expression analyses (Das et al., 2018).

The YO transcriptome of MLA-induced G. lateralis shows significant changes in global gene expression over the molt cycle (Fig. 5A). Of the 48,590 unique contigs catalogued in the filtered YO transcriptome, 28,179 (58%) are differentially expressed in pair-wise comparisons between sequential molt stages (Das et al., 2018). YO activation in early premolt is associated with major shifts, both up and down, in contig levels; 4,818 contigs are up-regulated and 11,324 are down-regulated in early premolt (Fig. 5B; IM to EP). By contrast, there is less change in gene expression from early premolt to mid-premolt; 283 contigs are upregulated and 89 contigs are down-regulated (Fig. 5B; EP to MP). A second major shift in gene expression occurs from mid-premolt to late premolt, when the committed YO achieves maximum ecdysteroidogenic capacity and the animal is preparing for ecdysis; 1,272 contigs are upregulated, while only 239 contigs are down-regulated (Fig. 5B; MP to LP). Interestingly, only about 10% of the 1,272 up-regulated contigs in late premolt are annotated (Fig. 5B). A large shift in gene expression occurs when the YO transitions from the committed state in late premolt to the repressed state in postmolt; 12,595 contigs are up-regulated and 5,534 contigs are down-regulated (Fig. 5B; LP to PM). Restoration of the basal state is associated with changes in the levels of 8,290 contigs; 3,852 are up-regulated and 4,438 are down-regulated (Fig. 5B; PM to IM). The differentially expressed genes in the pairwise comparisons are rarely the same, and the proportion of annotated and nonannotated contigs vary among the molt stages (Fig. 5B). Many of the contigs expressed at higher levels in the intermolt and premolt stages particularly signaling, cell growth, and ecdysteroidogenic genes - are expressed at very low levels in postmolt, suggesting that the repressed YO has reduced transcriptional activity (Fig. 3; Das et al., 2018). We hypothesize that these reduced transcript levels prevent YO activation until the exoskeleton is fully formed and hardened (Das et al., 2018). Thus, the basal, activated, committed, and repressed YO phenotypes are distinguished by unique transcriptomic assemblages that differ both qualitatively and quantitatively in contig levels.

The MLA YO transcriptome has 878 contigs mapped to 23 KEGG signaling pathways (Table 3). Over half (54%; 478 contigs) are differentially expressed over the molt cycle (Fig. 6; Das et al., 2018). The most common expression profile is high relative expression in intermolt, lower expression during premolt, and lowest expression in postmolt. Most of the MIH signaling genes show this expression profile (Fig. 7A). Seven of the 10 contigs are down-regulated in premolt; these include three adenylyl cyclases (Gl-ADCY), Gl-NOS, Gl-PKA, calcineurin (Gl-CALN), and Gl-PKG. Calmodulin (Gl-CALM) is up-regulated during premolt, while the expression of guanylyl cyclases Gl-GCI and Gl-GCIII are not affected by molt stage (Fig. 7A). All ten contigs are expressed at their lowest levels in postmolt. The down-regulation of MIH signaling genes in the activated YO precedes the reduced MIH sensitivity of the committed YO in mid- and late premolt (Chung and Webster, 2003;

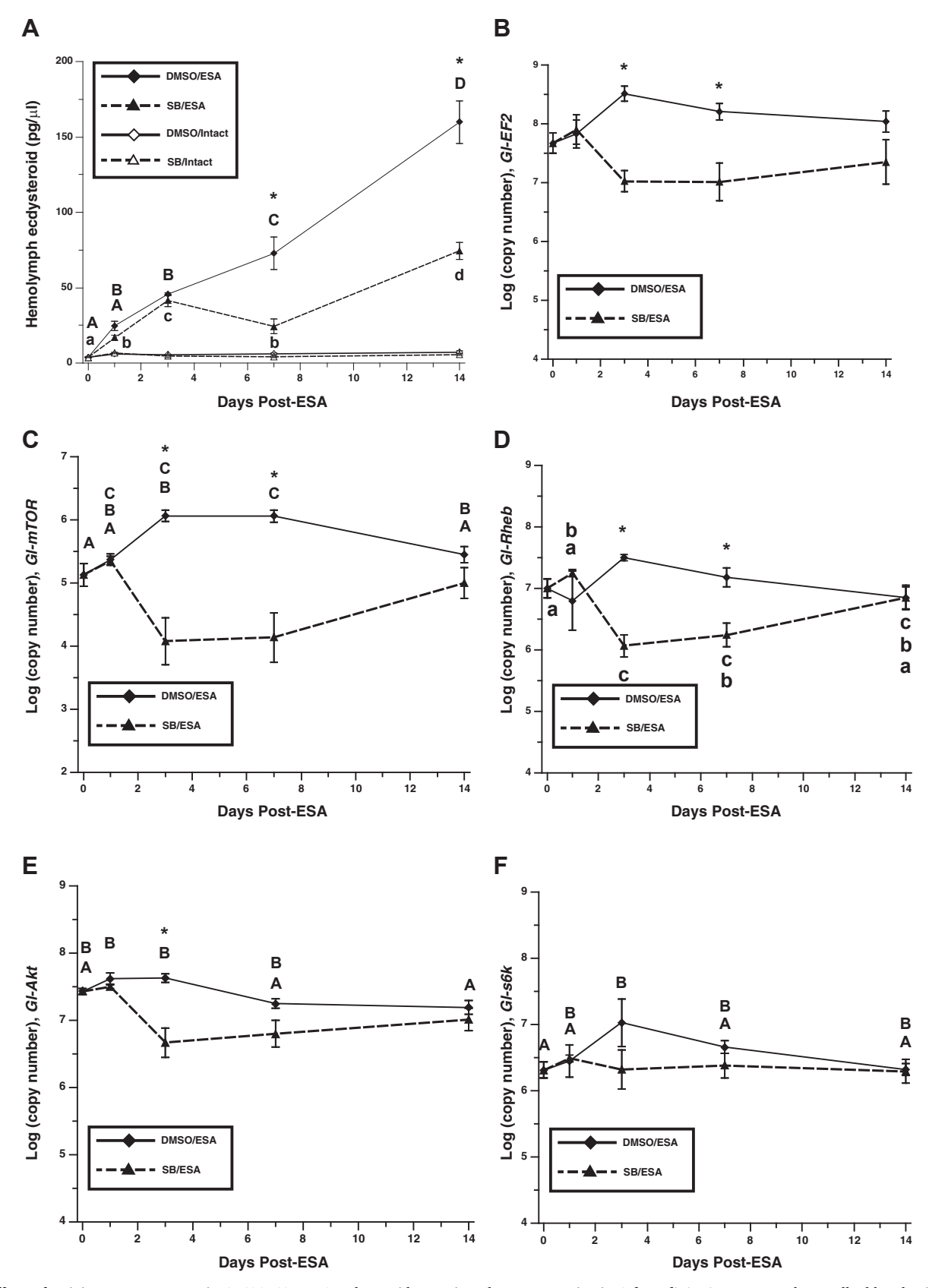


Fig. 4. Effects of activin receptor antagonist SB431542 on YO ecdysteroidogenesis and gene expression in *G. lateralis in vivo*. Intact and eyestalk-ablated animals were injected with a single dose of SB431542 in DMSO (\sim 10 μ M final hemolymph concentration) or DMSO (\sim 0.1% final hemolymph concentration) at Day 0. (A) Hemolymph ecdysteroid titer. Transcript levels of (B) *Gl-EF2*, (C) *Gl-mTOR*, (D) *Gl-Rheb*, (E) *Gl-Akt*, and (F) *Gl-S6K* were quantified by qPCR. Data are presented as mean \pm 1 s.e.m. (sample size for each treatment: Day 0, n = 8; Days 1, 3, and 7, n = 5; Day 14, n = 7). Asterisks indicate means that are significantly different (P < 0.05) between control and SB431542 at the same time point. Letters indicate significant differences in the means within a treatment (upper case for control; lower case for SB431542); means that are not significantly different share the same letter. Gene expression in intact animals was not measured. From Abuhagr et al. (2016).

Table 3Number of total and differentially expressed (DE) annotated contigs assigned to KEGG signal transduction pathways in the MLA *G. lateralis* YO transcriptome. From Das et al. (2018).

Signaling Pathway	Pathway ID	Number of annotated contigs	Number of DE contigs (percentage)
AMPK	k04152	86	53 (62%)
Calcium	k04020	92	49 (53%)
cAMP	k04024	104	65 (63%)
cGMP-PKG	k04022	94	51 (54%)
ErbB	k04012	48	24 (50%)
FoxO	k04068	79	46 (58%)
Hedgehog	k04340	36	21 (58%)
HIF-1	k04066	50	26 (52%)
Hippo	k04390	95	52 (55%)
Jak-STAT	k04630	26	12 (46%)
MAPK	k04010	106	66 (62%)
mTOR	k04150	92	54 (59%)
NF-kappa B	k04064	33	16 (48%)
Notch	k04330	28	17 (61%)
Phosphatidylinositol	k04070	86	47 (55%)
Phospholipase D	k04072	83	50 (60%)
PI3K-Akt	k04151	128	69 (54%)
Rap1	k04015	115	63 (55%)
Ras	k04014	105	57 (54%)
Sphingolipid	k04071	98	60 (61%)
TGF-beta	k04350	32	18 (56%)
TNF	k04668	40	23 (58%)
Wnt	k04310	79	51 (65%)

Nakatsuji and Sonobe, 2004; Nakatsuji et al., 2006; reviewed in Chang and Mykles, 2011; Nakatsuji et al., 2009). A second group of contigs are expressed at higher levels in intermolt and premolt and lower levels in postmolt (Fig. 6). This expression profile is shown by many of the contigs in the mTOR signaling pathway, such as Gl-mTOR, Gl-Raptor, Gl-Rictor, Gl-S6K, Gl-Akt, Gl-PTEN, Gl-STRADA, Gl-TSC2b, and Gl-Rheb (Fig. 7B). The combined effects of the down-regulation of the inhibitory contigs, such as Gl-TSC2a and Gl-EF4EBP, and the up-regulation of stimulatory contigs, such as Gl-Rheb and Gl-Akt, are consistent with increased mTORC1-mediated ecdysteroidogenesis during premolt. A third group is expressed at higher levels in early premolt. This expression profile is shown by components of the TGFβ/Activin signaling pathway (Fig. 7C; e.g., Gl-Mstn, Gl-Activin RI receptor, Gl-Smad2/3, and Gl-Smad4). Gl-BAMBI, an inhibitor of TGFB receptors, is down-regulated in all premolt stages (Fig. 7C). Components of other TGFB pathways, such as TGFβ/BMP signaling (Gl-BMP7, Gl-BMP receptor 1B (BMPR1B), Gl-Chordin (Gl-CHRD), Gl-Smad1, and Gl-Cul1), show highest expression in intermolt (Fig. 7C). This is consistent with the role of TGFβ/Activin signaling in YO commitment in mid-premolt (Abuhagr et al., 2016).

4.2. Effects of mTORC1 inhibitor rapamycin on the YO transcriptome

mTOR controls gene expression at transcriptional and translational levels (Saxton and Sabatini, 2017). As YO activation is associated with large changes in contig levels from intermolt to early premolt (Fig. 5; Das et al., 2018) and YO activation is inhibited by rapamycin (Fig. 3; Abuhagr et al., 2014b, 2016), we determined the effects of rapamycin on the YO transcriptome of *G. lateralis* induced to molt by ESA. Animals were ES-ablated and injected with either DMSO (Control group; \sim 0.1% DMSO final concentration) or rapamycin (Rapamycin group; \sim 10 μ M final concentration). YOs were harvested from intact (Day 0) animals and from control and rapamycin animals at 1, 3, and 7 days post-ESA with three technical replicates for each time point (Shyamal et al., 2018). A reference transcriptome of 69,002 contigs was *de novo*-assembled from over 1.066 billion reads from 21 cDNA libraries. Normalization by estimating library preparation artifacts of the RNA-seq data produced a filtered transcriptome of 35,696 contigs, 8,706 (24%)

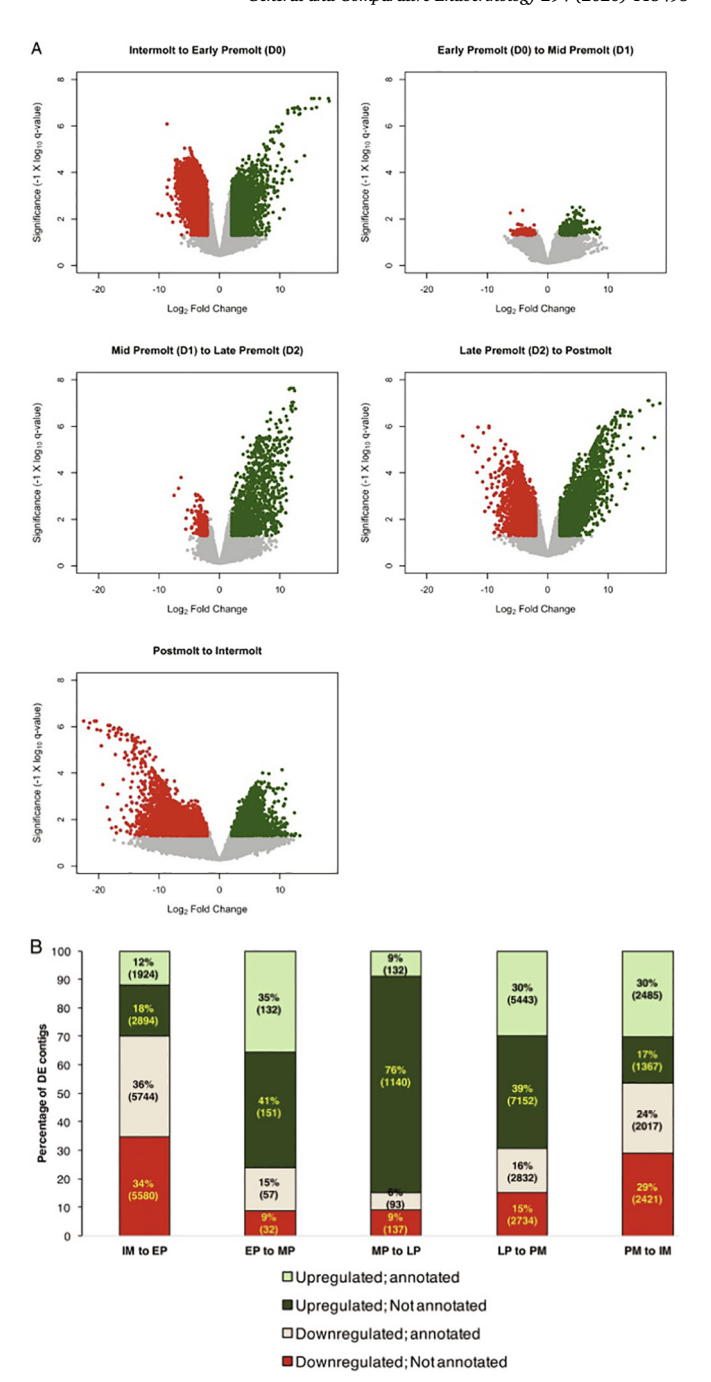


Fig. 5. Effects of molt stage on the levels of differentially-expressed (DE) contigs in the G. lateralis YO transcriptome. Animals were induced to molt by MLA. (A) Volcano plots of the DE contigs q-value as a function of log2 fold change. The cut-off used for identifying the DE contigs were: q-value < 0.05 and log2 fold change < -2 or > +2. The five pairwise comparisons used in this analysis are: intermolt (IM) to early premolt (EP); EP to mid-premolt (MP); MP to late premolt (LP); LP to postmolt (PM); and PM to IM. The DE contigs that have a negative fold change are indicated in red and DE contigs with a positive fold change are indicated in green. (B) Graphical representation of the number of DE contigs in each comparison. The number and percentage of annotated and not-annotated contigs are represented in green for up-regulated contigs and in red for down-regulated contigs. From Das et al. (2018).

of which are differentially expressed (Shyamal et al., 2018). Functional annotation assigned 4,887 contigs in the reference transcriptome to one or more KEGG pathways. These included 464 contigs assigned to 24 signal transduction pathways. The five highest number of assignments were to the mTOR, PI3K-Akt, $TGF\beta$, insulin, and Wnt signaling

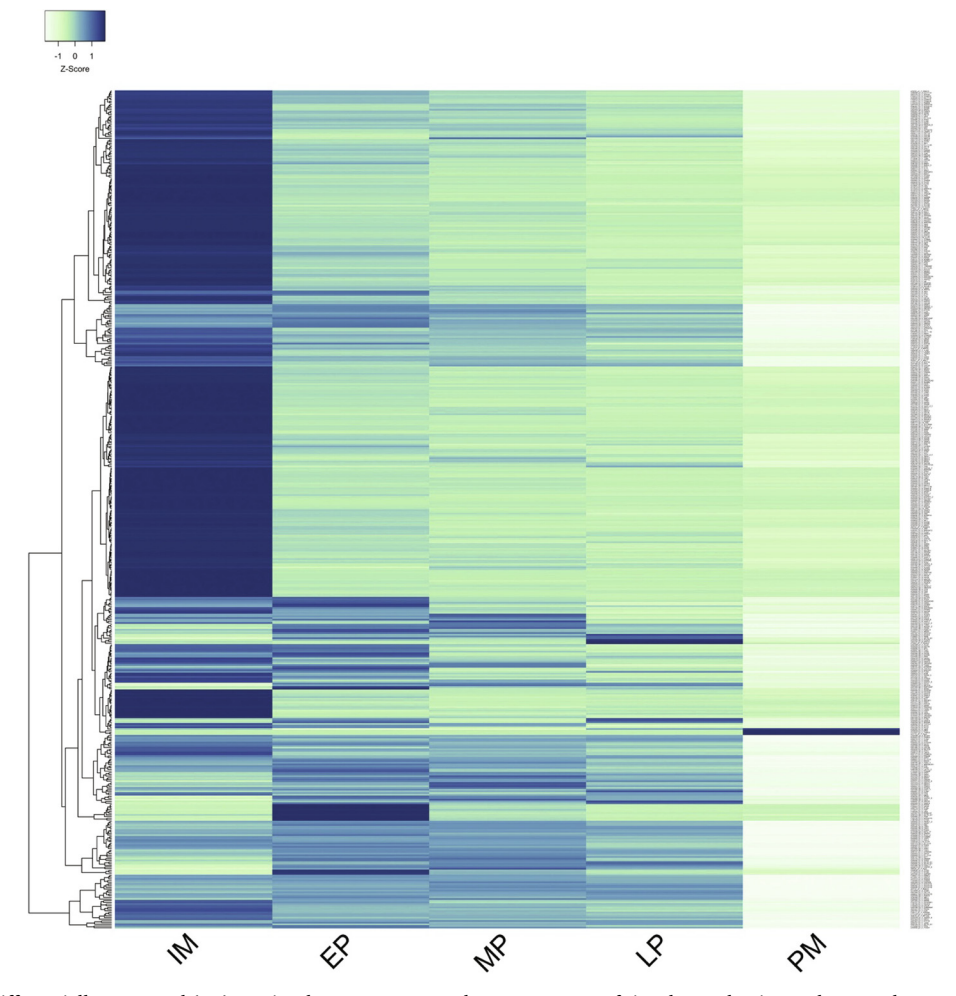


Fig. 6. Heatmap of 478 differentially expressed (DE) contigs that were annotated as components of signal transduction pathways. The average log FPKM values were used to show the expression profile of DE contigs across five molt cycle stages. The expression of the majority of the contigs was highest in IM and lowest in PM. Relatively fewer DE contigs were identified in the transitions from EP to MP and MP to LP. From Das et al. (2018). Abbreviations defined in the legend to Fig. 5.

pathways (Shyamal et al., 2018). The YO transcriptome also has contigs encoding enzymes in the insect juvenile hormone (JH) and ecdysteroid biosynthetic pathways (Shyamal et al., 2018; Sin et al., 2014; Tom et al., 2013).

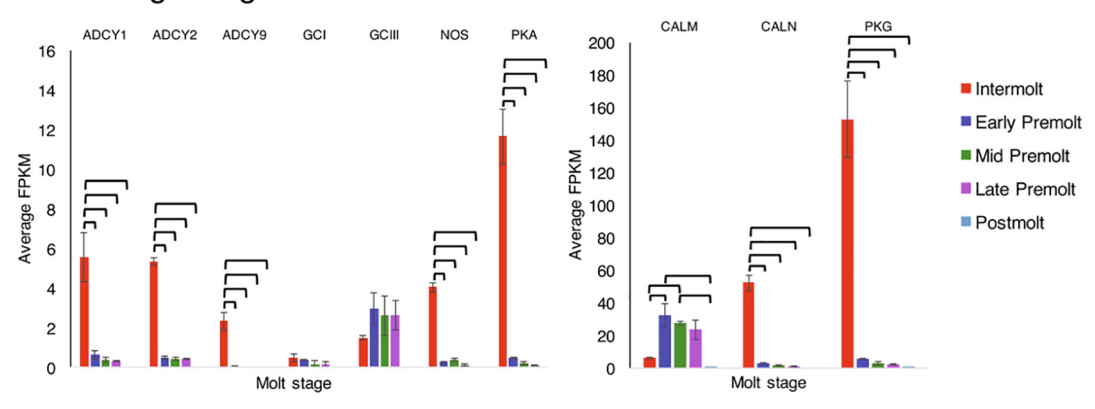
ESA results in large changes in global gene expression that are blocked by rapamycin. Interestingly, the largest differences between control and rapamycin-treated animals are at three days post-ESA; 3,104 genes are up-regulated, while 1,838 genes are down-regulated in control vs. rapamycin-treated YOs (Shyamal et al., 2018). This suggests that there is a delayed effect of mTOR inhibition on global gene expression.

Expression of MIH, mTOR, and TGFβ/Activin signaling genes are affected by ESA. Five adenylyl cyclases (*Gl-ADCY1*, *2*, *5*, *6*, and *9*), *Gl-NOS*, *Gl-PKA*, and *Gl-PKG* in the MIH pathway are down-regulated by ESA, while *Gl-CaM* and *GC-III* are up-regulated (Shyamal et al., 2018). mTORC1 signaling genes are up-regulated by ESA; these include *Gl-mTOR*, *Gl-Rheb*, *Gl-TSC1/2*, *Gl-Raptor*, *Gl-mLST8*, *Gl-Tel2*, *Gl-Akt*, *Gl-S6K*, and *Gl-S6* (Fig. 8A; Shyamal et al., 2018). Moreover, increased *Gl-eIF4E* and *Gl-EF2* contig levels indicate increased protein synthetic capacity induced by ESA (Shyamal et al., 2018). Interestingly, *Gl-FKBP12* is down-regulated by ESA, suggesting that the activated YO becomes insensitive to rapamycin (Shyamal et al., 2018). The down-regulation of MIH signaling genes and the up-regulation of mTOR signaling genes by ESA are comparable to the changes in the expression of MIH and mTOR signaling genes from intermolt to early premolt in MLA-induced animals (Das et al., 2018; see section 4.1 and Fig. 7A, B). Most of the

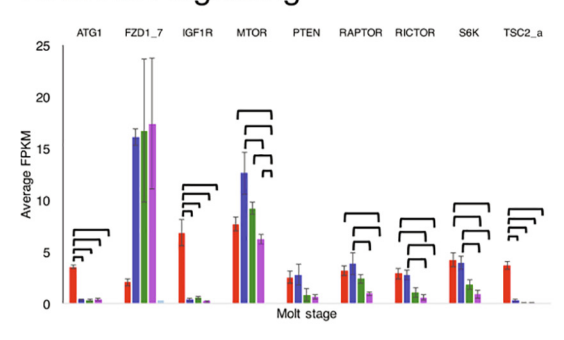
TGFβ/Activin signaling genes are down-regulated by ESA; these include *Gl-ACVR1*, *Gl-BAMBI*, *Gl-Smad2/3*, *Gl-Smad4*, and *Gl-Smad6*. *Gl-Mstn* contig level is not affected by ESA (Shyamal et al., 2018). These results are not consistent with previous results, which showed increased or sustained expression of *Gl-Mstn*, *Gl-ACVR1*, *Smad2/3*, *Gl-Smad4*, and *Gl-Smad6* in MLA- and ESA-induced animals (Abuhagr et al., 2016; Das et al., 2018; see section 4.1 and Fig. 7C). A possible explanation is that the animals in the ESA transcriptomic study failed to transition to the committed state by 7 days post-ESA, based on the hemolymph ecdysteroid titers (Shyamal et al., 2018). As the changes in contig levels are largely prevented or minimized by rapamycin (Fig. 8B; Shyamal et al., 2018), we conclude that mTOR activity controls, either directly or indirectly, the expression of MIH, mTOR, and TGFβ/Activin signaling genes in the activated YO.

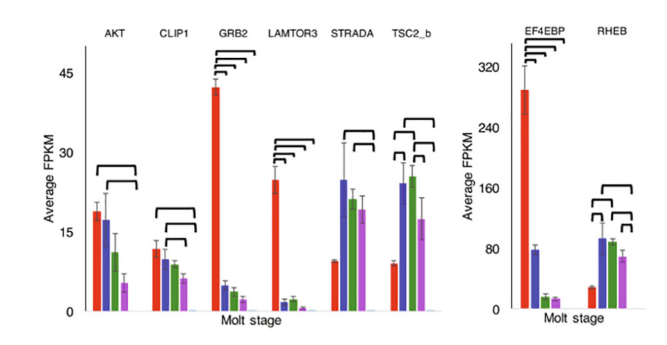
ESA alters the expression of genes in the insect hormone biosynthetic pathways. All five genes in the ecdysteroid synthetic pathway (Gl-Nvd, Gl-Spo, Gl-Phm, Gl-Dib, and Gl-Sad) are up-regulated by ESA and down-regulated by rapamycin (Shyamal et al., 2018). By contrast, the ten contigs in the JH biosynthetic pathway lack a consistent response to ESA: five are up-regulated, two are down-regulated, and three are unchanged (Shyamal et al., 2018). However, rapamycin blocks the ESA-induced changes in expression of the JH biosynthetic pathway genes (Shyamal et al., 2018). A critical enzyme in the pathway is juvenile hormone acid O-methyltransferase (JHAMT), which catalyzes the conversion of farnesoic acid to methylfarnesoate (MF). MF is the putative JH analog in crustaceans (Qu et al., 2018). Gl-JHAMT contig

A. MIH signaling

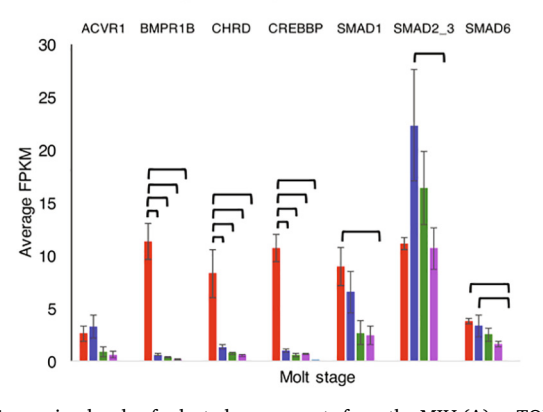


B. mTOR signaling





C. TGFB signaling



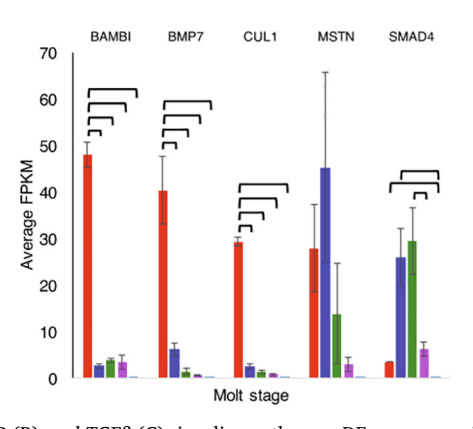


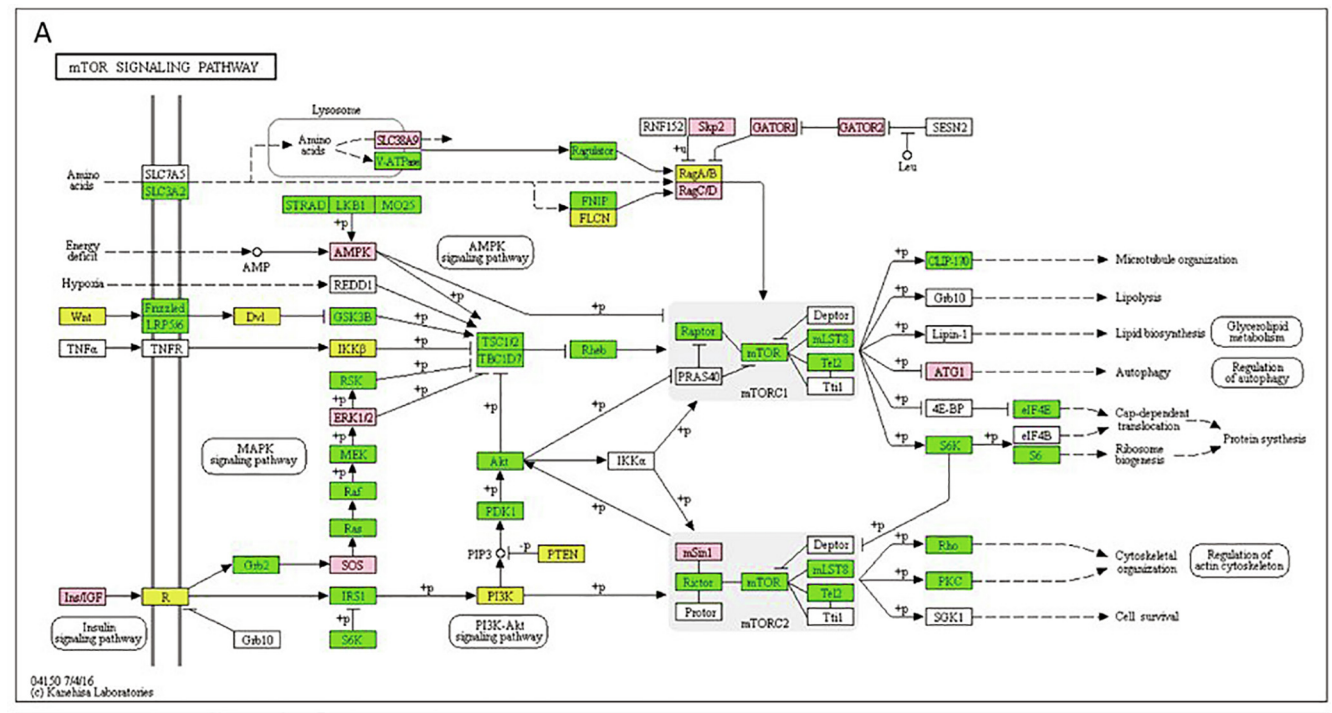
Fig. 7. Expression levels of selected components from the MIH (A), mTOR (B), and TGF β (C) signaling pathways. DE genes were identified via ANOVA and post-hoc Tukey test (P < 0.05). A total of 40 genes were selected from these three pathways, 34 of which were differentially expressed. Brackets indicate significant differences between means (P < 0.05). From Das et al. (2018).

level is highest in intermolt and is down-regulated by ESA (Shyamal et al., 2018). Interestingly, *Gl-JHAMT* contig levels are further decreased in rapamycin-injected animals, which suggests that the repression of *Gl-JHAMT* expression by rapamycin is not mediated by mTOR (Shyamal et al., 2018). These data indicate that mTOR regulates the expression of JH and ecdysteroid biosynthetic genes. The down-regulation of *Gl-JHAMT* suggests that the activated YO decreases synthesis of MF, while the up-regulation of ecdysteroidogenic pathway genes supports the high ecdysteroid synthesis by the YO during premolt.

4.3. Other signaling pathways in the Y-organ

In addition to MIH, mTOR, and TGFβ, other signaling pathways may

play a role in regulating the YO. Twenty-three KEGG signal transduction pathways are represented in the *G. lateralis* transcriptomes, which suggests that the YO can potentially respond to wide variety of ligands and factors (Tables 2, 3; Das et al., 2016, 2018; Shyamal et al., 2018). Moreover, crosstalk between multiple pathways enables the YO to integrate simultaneous signals to effect an appropriate response. The MIH pathway consists of three KEGG pathways (calcium, cAMP, and cGMP signaling; Tables 2, 3). More than half of the genes in 21 of the 23 KEGG pathways are differentially expressed over the molt cycle (Table 3; Das et al., 2018). Many of these pathways converge on mTOR to control ecdysteroid synthesis. Stressors, such as temperature or hypoxia, inhibit mTOR activity via AMPK and HIF-1 signaling by down-regulating Rheb (Salminen et al., 2016; Saxton and Sabatini, 2017). AMPK, which is activated by high AMP/ADP to ATP ratios, inhibits Rheb by activating



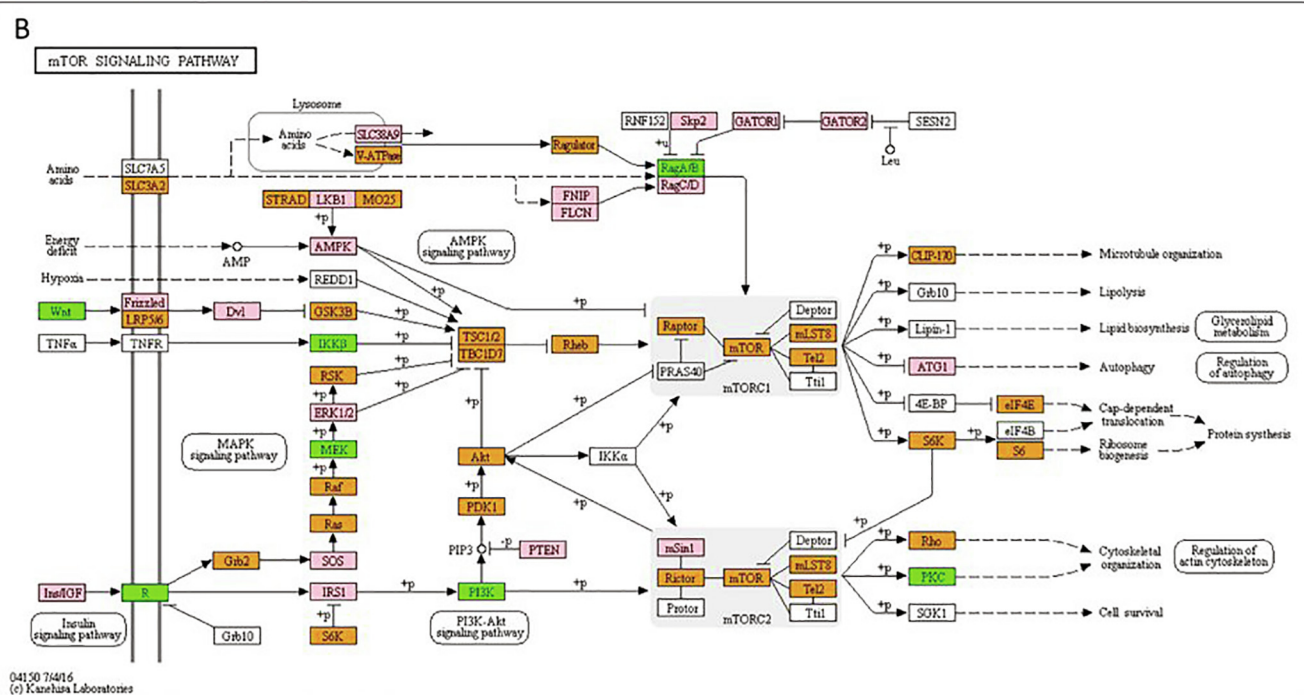


Fig. 8. Identification of genes assigned to the mTOR/WNT/AMPK signaling pathway in the *G. lateralis* YO/I/DRESA transcriptome. KAAS was used to identify genes annotated by BLAST against the specific insect databases and assigned to a KEGG pathway. Uncolored boxes were genes not assigned during annotation. Pink-colored boxes represent genes that show no change in expression levels. (A) Pairwise comparison of intact/intermolt vs ESA DMSO-control animals. Green colored boxes represent genes up-regulated in premolt relative to intermolt (intact); a yellow color indicates genes down-regulated when entering premolt relative to intermolt. (B) Pairwise comparison of ESA DMSO- and rapamycin-injected animals. Orange colored boxes indicate genes in premolt (DMSO-injected) that decrease in transcript abundance consequent to rapamycin treatment; green represents genes normally down-regulated when entering premolt that are now up-regulated by rapamycin treatment. From Shyamal et al. (2018).

TSC1/2 (Saxton and Sabatini, 2017). Growth factors, such as insulin, insulin-like growth factor (IGF), and epidermal growth factor, activate mTOR to stimulate cell growth (Cao et al., 2019; Kim and Guan, 2019; Liu and Sabatini, 2019; Saxton and Sabatini, 2017). Growth factors bind to receptor tyrosine kinases to stimulate MAPK and PI3K-Akt signaling pathways; phosphorylation of TSC1/2 by MAPK (ERK) and Akt inhibits TSC1/2, resulting in Rheb activation (Fig. 8; Saxton and

Sabatini, 2017).

Physiological studies using pharmacological reagents have shown that other signaling pathways can regulate YO ecdysteroidogenesis. These pathways are not activated by MIH. Reagents that increase intracellular Ca²⁺ can stimulate YO ecdysteroid secretion, while reagents that decrease or block Ca²⁺ signaling can inhibit YO ecdysteroid secretion (Mattson and Spaziani, 1986b, 1987; Sedlmeier and Seinsche,

1998; Spaziani et al., 1999, 2001). The Ca²⁺ ionophore A23187 stimulates YO ecdysteroid secretion in Cancer antennarius and crayfish, Orconectes limosus (Mattson and Spaziani, 1986b, 1987; Sedlmeier and Seinsche, 1998). As the A23187-induced increase in ecdysteroid secretion does not require extracellular Ca²⁺, A23187 releases Ca²⁺ from intracellular stores, such as the sarco/endoplasmic reticulum (SER) (Spaziani et al., 1999, 2001). However, the relatively high concentrations of A23187 used (10 and 100 μM) may have off-target effects. Interestingly, forskolin, which activates adenylyl cyclase, counters the A23187-induced increase (Mattson and Spaziani, 1986a, b). These results suggest that high intracellular Ca2+ stimulates a Ca2+/CaM-dependent PDE, such as PDE1 (Fig. 2; Francis et al., 2011; Peng et al., 2018); the reduced cyclic nucleotide levels stimulate ecdsyteroidogenesis (Mattson and Spaziani, 1986a; Spaziani et al., 1999). A SER Ca²⁺-ATPase (SERCA), which pumps Ca2+ from the cytosol to the SER lumen, is proposed to control intracellular Ca2+ levels over the molt cycle (Roegner et al., 2018, 2019). However, the expression pattern is not consistent with the changes in intracellular Ca2+, in which increases in intracellular Ca2+ are correlated with increased YO ecdysteroidogenesis in Callinectes sapidus (Chen et al., 2012; Chen and Watson, 2011). Although mRNA and protein levels are not necessarily correlated, if SERCA mRNA leads to an increase in SERCA protein, one would predict that the increased capacity by the SER to sequester Ca²⁺ would decrease, not increase, intracellular Ca2+ level during premolt. Moreover, Cs-SERCA mRNA level is lowest in the YO, when compared to hypodermis, hepatopancreas, and muscle (Roegner et al., 2019). ESA increases Ca2+ in the YO cells and causes a transient increase in Cs-SERCA mRNA level by 1 day post-ESA, suggesting that MIH is involved (Chen and Watson, 2011; Roegner et al., 2018). However, the response may be due to the acute reduction of other neuropeptides produced by the X-organ/sinus gland complex (Webster et al., 2012). There is no doubt that SERCA plays an important role in regulating intracellular Ca²⁺ in all cells, but there is no convincing evidence that SERCA is a component or target of the MIH signaling pathway. The effect of chronic elevation of Ca2+ on YO ecdysteroidogenesis by pharmacological reagents is most likely the result of activation of a Ca²⁺/CaMdependent PDE, such as PDE1, which hydrolyzes both cAMP and cGMP; the lower cyclic nucleotide levels de-repress the YO.

Phosphatidylinositol/Protein Kinase C (PKC) signaling stimulates YO ecdysteroidogenesis via a mechanism that is distinct from cAMP and Ca²⁺/CaM signaling (Spaziani et al., 2001). In the canonical pathway, ligand binding to a GPCR activates phospholipase C (PLC), which is mediated by a G_q protein. PLC hydrolyzes phosphatidylinositol to 1,2diacylglycerol (DAG) and inositol 1,4,5-trisphosphate (IP3), which triggers release of Ca2+ from intracellular stores. PKC is activated by the binding of Ca²⁺ and DAG. PKC activators, such as DAG synthetic analog 1-oleoyl-2-acetyl-glycerol, phorbol 12-myristate 13-acetate (PMA), and phorbol 12,13-dibutyrate stimulate ecdysteroidogenesis in the C. antennarius YO (Mattson and Spaziani, 1987). PMA counters the inhibitory effects of MIH, forskolin, dibutyryl cAMP, and PDE inhibitor IBMX (Mattson and Spaziani, 1987). Moreover, PMA does not counter the inhibitory effects of Ca2+ channel blocker lanthanum and CaM inhibitor trifluoperazine (Mattson and Spaziani, 1987). These data suggest that PKC activation is distinct from the MIH signaling pathway. The phosphatidylinositol signaling pathway is represented by 86 contigs in the G. lateralis YO transcriptome; 47 (55%) are differentially expressed over the molt cycle (Das et al., 2018). The ligand and GPCR involved in this pathway have not been identified.

A large number of GPCRs that bind a variety of neuropeptides are expressed in the YO. Sixty-six putative GPCRs have been identified in the *C. maenas* YO transcriptome and 99 GPCRs have been identified in the *G. lateralis* YO transcriptome (Oliphant et al., 2018; Tran et al., 2019). GPCRs have an extracellular ligand-binding domain, seven transmembrane α -helices, and a cytosolic domain (Buckley et al., 2016; Oliphant et al., 2018; Tran et al., 2019). Class A (rhodopsin-like) are the most abundant GPCRs expressed in the YO (59 in *C. maenas* and 49 in *G.*

lateralis), followed by Class B (secretin-like; 7 in C. maenas and 35 in G. lateralis), and Class C (metabotropic glutamate; 9 in G. lateralis) (Oliphant et al., 2018; Tran et al., 2019). Phylogenetic and in silico structural analysis identified 2 or 3 contigs encoding putative CHH family receptors related to insect ion transport peptide (ITP) receptors (Buckley et al., 2016; Oliphant et al., 2018; Tran et al., 2019; Veenstra, 2015). Three CHH GPCRs, designated Gl-GPCR-A9, -A10, and -A12, are expressed in the G. lateralis YO (Tran et al., 2019). Interestingly, other tissues do not express both Gl-GPCR-A9 and -A12 (The tissue distribution of Gl-GPCR-A10 was not determined). Gl-GPCR-A9 is expressed in evestalk ganglia, gill, heart, midgut, and thoracic ganglion, while Gl-GPCR-A12 is expressed in the hindgut, hepatopancreas, and testis: muscle does not express either gene (Tran et al., 2019). These results suggest that the YO responds to two CHH neuropeptides, eight tissues respond to either CHH neuropeptide, and that muscle responds to neither ligand. The expression of Gl-GPCR-A9 and Gl-GPCR-A12 in tissues other than the YO suggests that neither is a candidate for the MIH receptor, but further study is needed.

The expression of the corazonin (CRZ) receptor, another Class A GPCR, is restricted to the YO in C. maenas, suggesting that CRZ regulates YO function (Alexander et al., 2018; Oliphant et al., 2018). CRZ has diverse functions in insects, including the initiation of ecdysis behavior by releasing the neuropeptides pre-ecdysis triggering hormone and ecdysis triggering hormone from INKA cells in the brain of Manduca sexta larvae (Kim et al., 2004c). CRZ has no effect on ecdysteroid synthesis in intermolt and mid- and late premolt YOs, but does have a small stimulatory effect on ecdysteroid synthesis in postmolt YOs (Alexander et al., 2018). Two contigs encoding CRZ receptors, designated Gl-GPCR-A6 and -A7, are expressed in the G. lateralis YO (Tran et al., 2019). Gl-GPCR-A6 is not expressed in intermolt and early premolt, increases in mid- and late premolt, and reaches its highest level in postmolt (Tran et al., 2019). By contrast, Gl-GPCR-A7 is expressed at all molt stages (Tran et al., 2019). This expression pattern suggests that GPCR-A6 mediates the mild stimulatory effect of CRZ on YO ecdyster-

Leucine-rich repeats-containing GPCRs (LGRs) are members of the rhodopsin family of GPCRs. They are distinguished from other Class A GPCRs by having multiple repeats of leucine-rich sequences in the extracellular domain (Van Hiel et al., 2012). The G. lateralis YO transcriptome has five LGRs and the C. maenas YO transcriptome as nine LGRs (Oliphant et al., 2018; Tran et al., 2019). One of the LGRs, designated Gl-GPCR-A14b, may mediate the inhibition of the YO by LAF_{pro}, a peptide factor produced by secondary limb regenerates (Yu et al., 2002). Gl-GPCR-A14b clusters in the LGR3 clade. In Drosophila melanogaster, LGR3 is activated by Dilp8, which is an insulin-like peptide (ILP) produced by injured or damaged imaginal discs (Colombani et al., 2012; Garelli et al., 2012; Gontijo and Garelli, 2018; Jaszczak et al., 2016). Dilp8 inhibits ecdysteroidogenesis in the prothoracic gland by activating NOS (Jaszczak et al., 2015). Thus, NO inhibits ecdysteroidogenesis in the YO and insect prothoracic gland, with NOS activated by MIH and Dilp8, respectively. The data suggest that LAF_{pro} is an ILP and that Gl-GPCR-A14b is the LAF_{pro} receptor.

5. Proteomic analysis of the Y-organ over the molt cycle

Proteomic analyses of the YO are limited to the studies of two decapod species, *C. maenas* and *G. lateralis*. An early study examined the effects of ESA on the *G. lateralis* YO proteome using two-dimensional polyacrylamide gel electrophoresis (2D-PAGE). Of the 543 proteins that were quantified at 0, 1, and 3 days post-ESA, 170 proteins increase at least 3-fold and 89 proteins decrease at least 3-fold by ESA (Lee and Mykles, 2006). Three groups of phosphoproteins (\sim 12 kDa, \sim 17 kDa, and \sim 150 kDa) were isolated from cell extracts of 0 and 1 day post-ESA YOs, using a phosphoprotein column. The \sim 12 kDa protein is decreased, the \sim 17-kDa group is increased, and the \sim 150-kDa group is only present at 1 day post-ESA (Lee and Mykles, 2006). The \sim 150-kDa

group, which consisted of three proteins with different isoelectric points, was identified as NOS, using anti-NOS immunostaining of western blots and mass spectrometry (MS) of trypsin digests of the most abundant $\sim 150\text{-kDa}$ protein extracted from the gel (Lee and Mykles, 2006). A cDNA sequence encoding *Gl-NOS* made it possible to identify the $\sim 150\text{-kDa}$ phosphoprotein by comparing the masses of the trypsin digests with the masses of the peptides predicted from the deduced cDNA sequence (Kim et al., 2004a; Lee and Mykles, 2006). The different isoelectric points of the three $\sim 150\text{-kDa}$ proteins can be attributed to different degrees of phosphorylation. The identification of the other proteins was impractical at the time, as there were no transcriptome databases available for annotation.

More recent proteomic analysis has shown that the protein composition of the YO changes over the molt cycle. The YO protein compositions were examined in intermolt, early premolt (stage D₀), early postmolt (stage B), and late postmolt (stage C₁₋₃) C. maenas (Hamer, 2015) and in intermolt, early premolt, mid-premolt (stage D₁), and late premolt (stage D₂) G. lateralis (Head et al., 2019). Proteins were separated by 2D-PAGE and each protein was digested with trypsin and analyzed by tandem MS. The assignment of trypsin peptides to specific proteins was aided by the annotated transcriptome from the G. lateralis YO. A total of 457 proteins were analyzed in the G. lateralis YO (Fig. 9); 230 (50%) proteins changed in abundance over the molt cycle. Of the 191 proteins identified by tandem MS, 109 (47%) changed in abundance and were assigned to functional categories (Head et al., 2019). A total of 279 proteins were analyzed in the C. maenas YO and 91 (33%) were identified (Hamer, 2015). Twenty-four of the 91 identified proteins changed in abundance in at least one of the molt stages relative to the others (Hamer, 2015). The lower identification rate is attributed to the fact that the C. maenas YO transcriptome database was not available at that time (Hamer, 2015).

The results from the assignment of the differentially-expressed proteins into functional categories are summarized in Fig. 10. The changes in the functional categories is consistent with the changes in the YO over the molt cycle (Head et al., 2019). The basal YO is characterized by basal energy metabolism, radical oxygen species (ROS) scavenging, and protein degradation protein categories. By early premolt, the activated YO is characterized by functional categories associated with YO hypertrophy and ecdysteroid synthesis and secretion: increased energy metabolism, cytoskeleton, vesicular secretion, amino acid metabolism, and immune response proteins. In addition, the increases in the abundances of hemocyanin and cryptocyanin parallel the increases of these proteins in the hemolymph (Head et al., 2019). By

mid-premolt, the predominant categories in the committed YO are energy metabolism, ROS scavenging, cytoskeleton, vesicular secretion, immune response, and protein homeostasis and turnover proteins. By late premolt, energy metabolism, ROS scavenging, and protein homeostasis proteins are dominant. The high levels of ROS scavenging proteins, such as manganese superoxide dismutases, catalase, and peroxiredoxins, neutralize oxygen radicals produced from hydroxylation reactions catalyzed by cytochrome P450 Halloween enzymes and from cytochromes in the mitochondrial electron transport chain (Hamer, 2015; Head et al., 2019; Hrycay and Bandiera, 2015). A transaldolase, which may regulate ecdysteroidogenesis (Lachaise et al., 1996) and glutamate dehydrogenase, which converts glutamate to α -ketoglutarate to activate mTOR (Duan et al., 2015; Wu et al., 2016), increase during premolt (Head et al., 2019). The repressed YO in postmolt G. lateralis was not analyzed (Head et al., 2019). Principle component (PC) analysis of the proteins that significantly changed in the C. maenas YO showed that the intermolt and early premolt stages were separated from the early and late postmolt stages along the PC1 axis, which were represented by differences in the abundances of cytoskeleton, ROS scavenging, and hemolymph proteins (Hamer, 2015). A PC analysis of the G. lateralis proteome revealed distinct intermolt, early premolt, midpremolt, and late premolt clusters (Head et al., 2019). These results indicate that the basal, activated, committed, and repressed YO are distinguished by qualitative and quantitative changes in protein abundance that are associated with YO functional properties. An important discovery was the increased levels of ROS scavenger proteins to counter the effects increased energy production and ecdysteroid synthesis in the premolt YO.

6. Conclusions and perspectives

Progress over the last ten years has identified signaling mechanisms that regulate the YO and has provided a fresh perspective on earlier work. The model for the organization of the MIH, mTOR, and TGFβ/Activin signaling pathways is presented in Fig. 11. mTOR has a central position, as it is regulated by MIH and most likely other signaling pathways, as it controls the allocation of energy and nutrients for protein, lipid, and nucleic acid synthesis (Cao et al., 2019; Kim and Guan, 2019; Liu and Sabatini, 2019; Saxton and Sabatini, 2017; Weichhart, 2018). mTOR controls the activation of the YO in early premolt, as ecdysteroidogenesis is inhibited by rapamycin *in vivo* and *in vitro* (Fig. 3; Abuhagr et al., 2014b). mTOR acts initially by phosphorylating 4EBP and S6K to stimulate the translation of mRNA, as

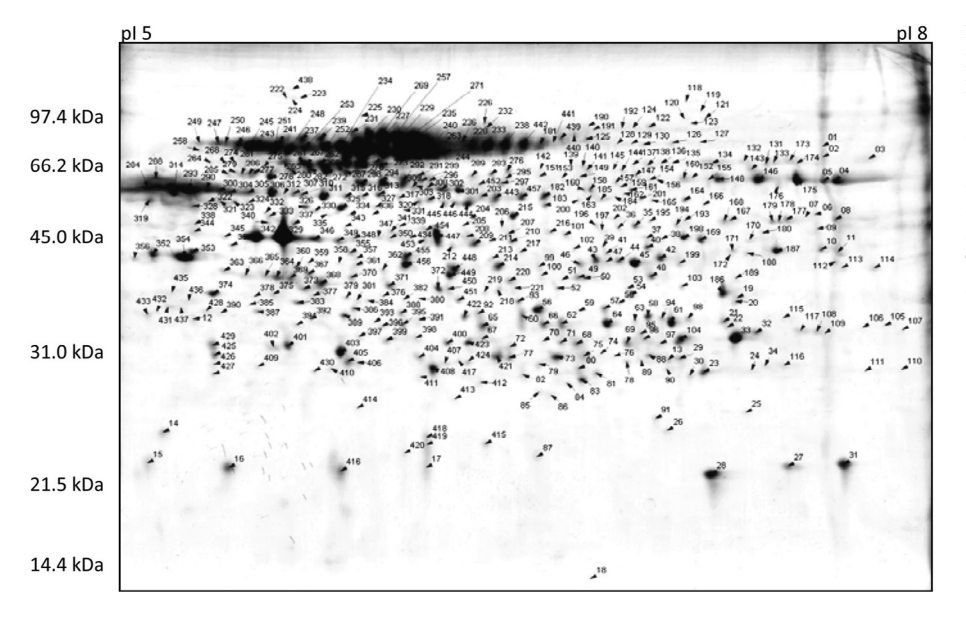


Fig. 9. Two-dimensional gel proteome map composed of gels from all molt stages. Spot numbers represent all 457 protein spots detected from the *G. lateralis* YO in intermolt, early, mid-, and late premolt stages. The average pixel density from this fused image was normalized to determine changes in pixel density (protein abundance) among each gel image in each molt stage. All protein spots were manually excised from gels for identification using MALDI-ToF/Tof mass spectrometry, of which 191 were positively identified. From Head et al. (2019).

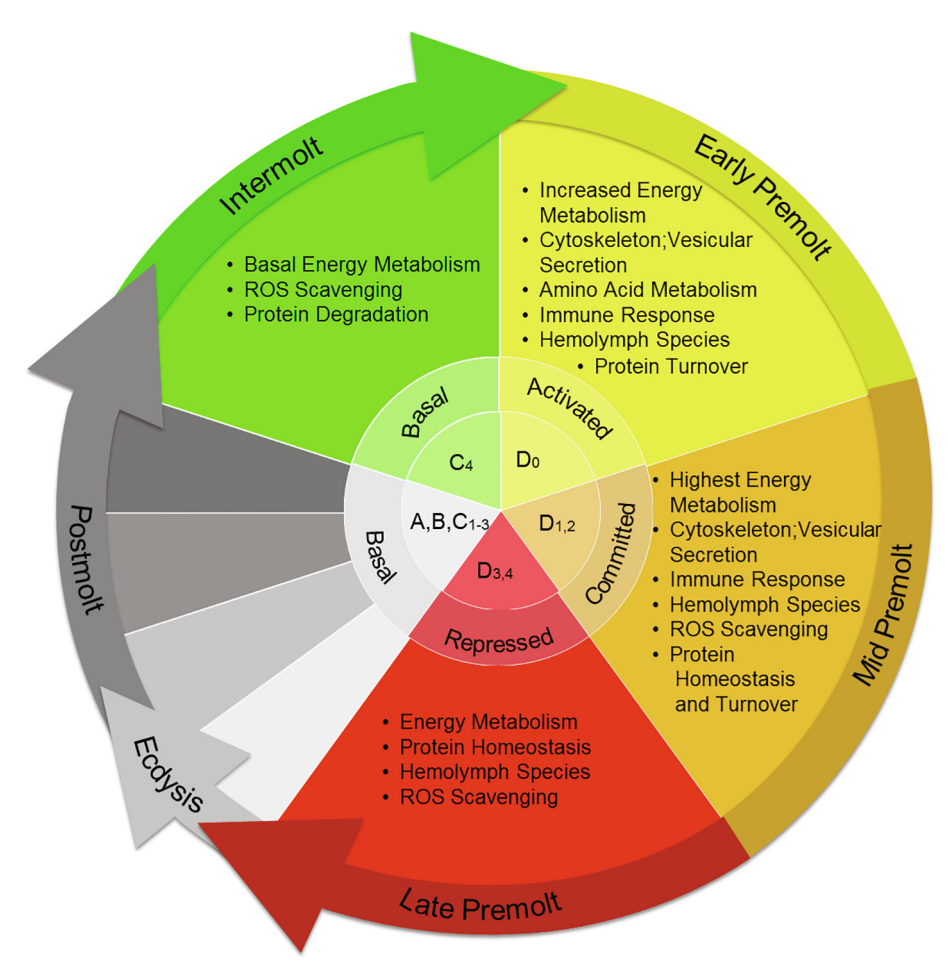


Fig. 10. Summary of the major functional categories of proteins at each molt stage in the *G. lateralis* YO. Inner circles represent the molt stage abbreviation and physiological state of the YO. Proteomic analysis of postmolt crabs were not conducted. From Head et al. (2019).

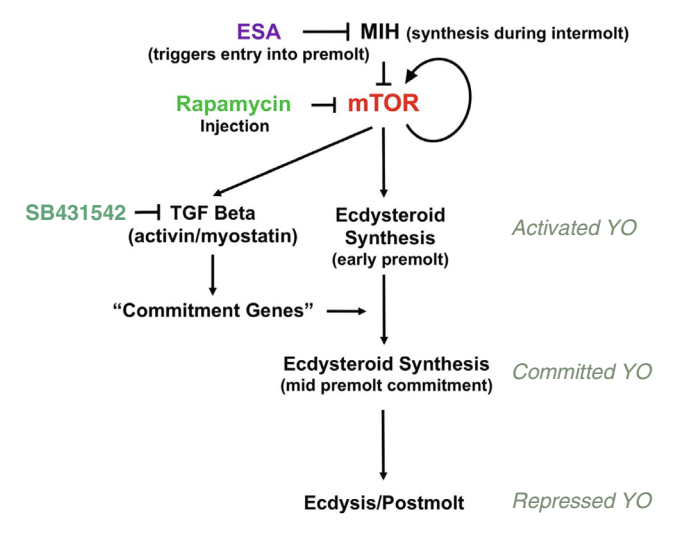


Fig. 11. Organization of the signaling pathways mediating YO phenotype transitions over the molt cycle. Cyclic nucleotide-mediated MIH signaling maintains the YO in the basal state by inhibiting mTOR signaling. Reduction in MIH, such as eyestalk ablation (ESA), stimulates mTOR activity, which is inhibited by rapamycin. mTOR stimulates ecdysteroid synthesis and up-regulates mTOR and TGF β /Activin signaling genes, and down-regulates MIH signaling genes. Activin/myostatin signaling, which is inhibited by SB431542, up-regulates mTOR signaling genes and controls expression of commitment genes that determine the committed phenotype. High ecdysteroid titers in late premolt may trigger the repressed phenotype in postmolt. Modified from Shyamal et al. (2018).

rapamycin inhibits YO ecdysteroid secretion (Abuhagr et al., 2014b) and cycloheximide, but not actinomycin D, inhibit YO ecdysteroidogenesis and protein synthesis *in vitro* (Covi et al., 2009; Dauphin-Villemant et al., 1995; Han et al., 2006; Mattson, 1986; Mattson and Spaziani, 1987). Cycloheximide also inhibits the uptake of high-density lipoprotein in the *C. antennarius* YO, suggesting that mTOR activity is also necessary for the uptake of cholesterol for ecdysteroid synthesis (Kang and Spaziani, 1995). Moreover, YO protein synthesis is increased during premolt (Dauphin-Villemant et al., 1995; Mykles, 2011). These results provide strong evidence that mTOR-dependent protein synthesis is necessary for the increase in ecdysteroid synthesis in the activated YO. mTOR activity acts at the translational level to drive the transition of the YO from the basal to activated state (Figs. 1, 11).

mTOR is also necessary to support further increases in YO ecdysteroid synthesis in mid- and late premolt animals. Increased hemolymph ecdysteroid titers are correlated with increased YO ecdysteroid synthesis and secretion (see Mykles, 2011 for references). Hypertrophy of the YO is accompanied by the proliferation of mitochondria and elaboration of the SER (Kang and Spaziani, 1995; Lachaise et al., 1993; Shyamal et al., 2014), which corresponds to increases in energy metabolism and ROS scavenging proteins (Head et al., 2019). This increases ecdysteroid synthetic capacity, as cytochrome P450 enzymes that catalyze the ecdysteroid synthetic reactions are localized in the mitochondrion or SER (Lachaise et al., 1993; Mykles, 2011). This appears to be controlled at the transcriptional level by mTOR. RNA-seq data show that mTOR activity regulates the mRNA levels of thousands of genes by three days post-ESA (Shyamal et al., 2018). Three notable pathways are up-regulated by mTOR: mTOR signaling itself, TGFβ/ Activin signaling, and the ecdysteroid synthetic pathway. Up-regulation

of mTOR signaling genes in early premolt in MLA animals (Fig. 7B) and by ESA (Figs. 4, 8) constitutes a positive feedback mechanism that would drive the YO forward in the molt cycle (Fig. 11). Up-regulation of TGFβ/Activin signaling by mTOR is necessary for YO commitment, as rapamycin not only inhibits YO activation, it also prevents transition of the YO to the committed state (Fig. 3). ESA increases Gl-Mstn mRNA levels by 3 days post-ESA (Abuhagr et al., 2016). YO commitment involves changes in gene expression mediated by Smad transcription factors activated by Mstn/Activin (Fig. 11). TGFβ/Activin up-regulates mTOR signaling, as SB431542 decreases the mRNA levels of Gl-mTOR, Gl-Rheb, Gl-Akt, and Gl-EF2 by three days post-ESA and lowers hemolymph ecdysteroid titers by seven days post-ESA (Fig. 4), ESA-induced increases in ecdysterodogenic pathway genes are inhibited by rapamycin (Shyamal et al., 2018). These data suggest that transcriptional control by TGFB/Activin signaling precedes the large increase in ecdysteroid synthesis in mid- and late premolt. Other than the mTOR signaling genes, the Mstn/Activin gene targets, designated "commitment genes" (Fig. 11), have yet to be identified. Taken together, gene regulation by mTOR supports the synthesis of macromolecules needed for YO hypertrophy, supports YO activation, and drives the Mstn/Activin-mediated transition of the YO from the activated to committed state (Figs. 1, 11).

The interaction between MIH and mTOR signaling pathways contributes to the changes in physiological properties of the YO in the intermolt and premolt stages. MIH signaling maintains the YO in the basal state by inhibiting mTOR-dependent protein synthesis necessary for sustained ecdysteroidogenesis (Fig. 11). The MIH signaling model explains how prolonged inhibition of the YO is accomplished by the pulsatile release of MIH from the X-organ/sinus gland. A Ca2+/CaMdependent NOS plays a critical role by linking a transient increase in cAMP to the sustained production of cGMP by GC-I (Fig. 2). Protein synthesis is inhibited by MIH or sinus gland extracts (Dauphin-Villemant et al., 1995; Mattson and Spaziani, 1986b), Cell-permeable cyclic nucleotide analogs, forskolin, and PDE inhibitor IBMX inhibit YO ecdysteroidogenesis and protein synthesis (Covi et al., 2009; Han et al., 2006; Han and Watson, 2005; Mattson, 1986; Mattson and Spaziani, 1986b, 1987; Webster et al., 2012). Once activated, mTOR activity leads to the down-regulation of MIH signaling genes. This, coupled with increased PDE activity, contributes to the decreased sensitivity of the YO in mid- and late premolt.

Two critical questions regarding the MIH signaling pathway remain to be answered: (1) What is the identity of the MIH/CHH receptor(s)? and (2) How does PKG inhibit mTOR activity? Some progress has been made in answering the first question. Several putative CHH GPCRs have been identified in the YO using transcriptomics and in silico analyses (Tran et al., 2019). The next step is to develop functional assays to determine ligand binding properties and specificities. One approach is to transiently express candidate GPCRs in a heterologous reporting system to test recombinant MIH and CHH (Ventura et al., 2017). Although MIH and CHH share a similar structure (Katayama et al., 2003), they bind to distinct receptors in the YO membrane (Webster, 1993). This suggests that the two neuropeptides bind distinct GPCRs. However, this contradicts earlier work on hepatopancreatic membrane preparations that the CHH receptor is a membrane guanvlyl cyclase (GC-II: reviewed in Chang and Mykles, 2011; Covi et al., 2009, 2012). In order to answer the second question, the substrates of PKG must be identified and then determine which of those substrates inhibit mTOR. A likely downstream target is TSC1/2, which is inactivated by phosphorylation by Akt. PKG may phosphorylate and activate Akt, leading to the stimulation of mTOR by Rheb-GTP. A promising approach is to use liquid chromatography tandem MS to determine the effects of molt stage, ESA, and PKG inhibitors on the YO phospho-proteome.

The mechanisms for the transition of the YO from committed state to the repressed state and from the repressed state back to the basal state remain to be elucidated. The peak in hemolymph ecdysteroid titers in late premolt may initiate the transition to the repressed

phenotype. The transition from very high to very low ecdysteroid synthesis occurs over a relatively short period, from the end of late premolt to as little as one day post-ecdysis. This results in very low hemolymph ecdysteroid titers in postmolt (Mykles, 2011). By 10 days postmolt in G. lateralis, the levels of most contigs, including those in the MIH, mTOR, and TGFβ/Activin signaling pathways, are at their lowest levels, suggesting that the repressed YO is transcriptionally inactive (Fig. 7; Das et al., 2018). The down-regulation of MIH signaling genes suggests that the insensitivity of the committed YO to MIH continues in the repressed YO. If so, YO repression would not involve MIH signaling. The repressed phenotype is distinct from the basal phenotype and prevents molting until the new exoskeleton is completely formed (Das et al., 2018). The repressed state is also distinct from the blocked state. in which the MIH signaling genes are up-regulated, but mTOR signaling genes are not affected (Pitts et al., 2017). The down-regulation of mTOR and TGFβ /Activin signaling pathways may keep the YO in the repressed state. Accordingly, not until the basal phenotype is restored in intermolt does normal control of YO ecdysteroidogenesis by MIH resume. Discovery of the mechanisms driving the transition from the repressed to basal state is a promising area for future research.

Transcriptomic and proteomic tools have contributed to a better understanding of the endocrine regulation of molting in decapod crustaceans. Five discrete YO phenotypes have been characterized, as best illustrated in the model species, G. lateralis. The YO progresses through the basal, activated, committed, and repressed states during a normal molt cycle (Fig. 1). The blocked phenotype occurs in those individuals or species that exit the molt cycle for an indefinite period, such as terminal anecdysis. Each phenotype has unique mRNA and protein profiles (Das et al., 2018; Head et al., 2019; Pitts et al., 2017). The MIH signaling, mTOR signaling, and TGFβ/Activin signaling pathways determine the basal, activated, and committed states, respectively, and high ecdysteroid may determine the repressed state (Fig. 11). Other signaling pathways are likely involved. A surprising discovery was that the G. lateralis YO transcriptome has 878 contigs assigned to 23 KEGG signaling pathways (Table 3; Das et al., 2018). For the GPCRs alone, the YO can potentially respond to dozens of ligands, ranging from biogenic amines (e.g., serotonin and octopamine) to various neuropeptides (e.g., MIH, CHH, LAF_{pro}, CRZ, allatostatins, bursicon, proctolin, and FMRFamides; Tran et al., 2019). This suggests that the YO resembles the insect prothoracic gland, which responds to a variety of tropic and static factors (Covi et al., 2012; Marchal et al., 2010; Rewitz et al., 2013; Yamanaka et al., 2013). Studies on insects suggest that Wnt and Hedgehog signaling regulate the prothoracic gland (Archbold et al., 2014; Rodenfels et al., 2014). Contigs of two Wnt ligands, Gl-Wnt5 and Gl-Wnt7, are at their highest levels in the YO of late premolt animals, suggesting that Wnt signaling is involved in the transition of the YO from the committed to the repressed state (Das et al., 2018). There is extensive crosstalk between mTOR, TGFB, MAPK, Jak-STAT, Wnt, Hippo, Notch, and Hedgehog pathways (Alexandratos et al., 2016; Andersen et al., 2013; Rewitz et al., 2013; Shimobayashi and Hall, 2014; Zhang et al., 2014), raising the possibility that the YO integrates a variety of signals to modulate ecdysteroidogenesis in response to variety of intrinsic and extrinsic factors.

High-throughput sequencing and tandem MS methods are transforming crustacean endocrinology (Das and Mykles, 2016; Mykles et al., 2016; Ventura et al., 2018; Head et al., 2019). The growing number of genomic and transcriptomic databases are resources for understanding phenotypic plasticity (Jung et al., 2013; Mykles et al., 2010b; Nong et al., 2020; Ventura et al., 2018; Zhang et al., 2019). The blackback land crab, *G. lateralis*, has proven to be a valuable model for experimental studies on the endocrine control of molting. However, *G. lateralis* and most other decapod species have limited usefulness for testing gene function. The only method available currently is dsRNA, which lacks tissue specificity and can have off-target effects (Sagi et al., 2013). The cherry shrimp, *Neocaridina davidi* (formerly *N. denticulata*) has many of the life history traits that make it a suitable model

organism for functional genomics (Mykles and Hui, 2015). Until a transgenic model is developed, crustacean biologists must continue to rely on dsRNA knockdown experiments to determine gene function.

Acknowledgements

The authors thank the many students, technicians, postdoctoral fellows, visiting scientists, and collaborators who contributed to this work. In particular, we acknowledge Sharon Chang and Dr. Sukkrit Nimitkul, UC Davis Bodega Marine Laboratory; Dr. Ali Abuhagr, Dr. Samiha Benrabaa, Dr. Joseph Covi, Dr. Sunetra Das, Dr. Hyun-woo Kim, Dr. Kara Lee, Dr. Sung Gu Lee, Dr. Alejandro López-Cerón, Megan (Mudron) Hines, Dr. Kyle MacLea, Audrey McDonald, Dr. Scott Medler, Dr. Natalie Pitts, Dr. Nada Rifai, Lindsay Vraspir, Dr. Astrid Wittmann, Dr. Xiaoli Yu, and Dr. Wen Zhou, Colorado State University; Dr. David Durica and Dr. Sharmishtha Shyamal, University of Oklahoma; Dr. Lars Tomanek, Mark Hamer, and Talia Head, California Polytechnic University, San Luis Obispo; and Dr. Tomer Ventura, University of the Sunshine Coast. We thank Hector Horta and Rafael Polanco for supplying *G. lateralis*. The authors acknowledge the support of grants from the California and Connecticut Sea Grant College Programs, the National Institutes of Health, and the National Science Foundation.

References

- Abuhagr, A.M., Blindert, J.L., Nimitkul, S., Zander, I.A., LaBere, S.M., Chang, S.A., et al., 2014a. Molt regulation in green and red color morphs of the crab Carcinus magnas: gene expression of molt-inhibiting hormone signaling components. J. Exp. Biol. 217, 796-808. https://doi.org/10.1242/jeb.093385.
- Abuhagr, A.M., MacLea, K.S., Chang, E.S., Mykles, D.L., 2014b. Mechanistic target of rapamycin (mTOR) signaling genes in decapod crustaceans: Cloning and tissue expression of mTOR, Akt, Rheb, and p70 S6 kinase in the green crab, Carcinus maenas, and blackback land crab, Gecarcinus lateralis. Comp. Biochem. Physiol. 168A, 25-39. https://doi.org/10.1016/j.cbpa.2013.11.008.
 Abuhagr, A.M., MacLea, K.S., Mudron, M.R., Chang, S.A., Chang, E.S., Mykles, D.L., 2016.
- Roles of mechanistic target of rapamycin and transforming growth factor-beta signaling in the molting gland (Y-organ) of the blackback land crab, Gecarcinus lateralis. Comp. Biochem. Physiol. 198A, 15-21. https://doi.org/10.1016/j.cbpa.2016.03.018.
- Alexander, J.L., Oliphant, A., Wilcockson, D.C., Audsley, N., Down, R.E., Lafont, R., et al., 2018. Functional characterization and signaling systems of corazonin and red pigment concentrating hormone in the green shore crab, Carcinus maenas. Frontiers Neurosci. 11, 752. https://doi.org/10.3389/fnins.2017.00752.

 Alexandratos, A., Moulos, P., Nellas, I., Mavridis, K., Dedos, S.G., 2016. Reassessing ec-
- dysteroidogenic cells from the cell membrane receptors' perspective. Sci. Rep. 6, 20229. https://doi.org/10.1038/srep20229.
- Andersen, D.S., Colombani, J., Leopold, P., 2013. Coordination of organ growth: principles and outstanding questions from the world of insects. Trends Cell Biol. 23, 336–344. https://doi.org/10.1016/j.tcb.2013.03.005.
- Archbold, H.C., Broussard, C., Chang, M.V., Cadigan, K.M., 2014. Bipartite recognition of DNA by TCF/pangolin is remarkably flexible and contributes to transcriptional responsiveness and tissue specificity of wingless signaling. PLoS Genetics. 10, e1004591. https://doi.org/10.1371/journal.pgen.1004591.
- Bliss, D.E., 1979. From sea to tree Saga of a land crab. Am. Zool. 19, 385-410.
- Buckley, S.J., Fitzgibbon, Q.P., Smith, G.G., Ventura, T., 2016. In silico prediction of the G-protein coupled receptors expressed during the metamorphic molt of Sagmariasus verreauxi (Crustacea: Decapoda) by mining transcriptomic data: RNA-seq to repertoire. Gen. Comp. Endocrinol. 228, 111–127. https://doi.org/10.1016/j.ygcen
- Budi, E.H., Duan, D., Derynck, R., 2017. Transforming growth factor-beta receptors and smads: Regulatory complexity and functional versatility. Trends Cell Biol. 27 658-672. https://doi.org/10.1016/j.tcb.2017.04.005.
- Cao, Y.C., Liu, S.M., Liu, K., Abbasi, I.H.R., Cai, C.J., Yao, J.H., 2019. Molecular mechanisms relating to amino acid regulation of protein synthesis. Nutrition Res. Rev. 32, 183–191. https://doi.org/10.1017/s0954422419000052.
- Chang, E.S., 1985. Hormonal control of molting in decapod Crustacea. Am. Zool. 25, 179-185.
- Chang, E.S., 1989. Endocrine regulation of molting in Crustacea. Rev. Aquatic Sci. 1, 131-158.
- Chang, E.S., Bruce, M.J., 1980. Ecdysteroid titers of juvenile lobsters following molt induction. J. Exp. Zool. 214, 157–160.
 Chang, E.S., Mykles, D.L., 2011. Regulation of crustacean molting: A review and our
- perspectives. Gen. Comp. Endocrinol. 172, 323-330.
- Chen, H.Y., Dillaman, R.M., Roer, R.D., Watson, R.D., 2012. Stage-specific changes in calcium concentration in crustacean (Callinectes sapidus) Y-organs during a natural molting cycle, and their relation to the hemolymphatic ecdysteroid titer. Comp. Biochem. Physiol. 163A, 170-173. https://doi.org/10.1016/j.cbpa.2012.05.205
- Chen, H.Y., Watson, R.D., 2011. Changes in intracellular calcium concentration in crustacean (*Callinectes sapidus*) Y-organs: Relation to the hemolymphatic ecdysteroid titer. J. Exp. Zool. 315A, 56-60. https://doi.org/10.1002/jez.646.
- Cheng, J.-H., Chang, E.S., 1991. Ecdysteroid treatment delays ecdysis in the lobster, Homarus americanus. Biol. Bull. 181, 169-174.

- Chung, J.S., Webster, S.G., 2003. Moult cycle-related changes in biological activity of moult-inhibiting hormone (MIH) and crustacean hyperglycaemic hormone (CHH) in the crab, Carcinus maenas. From target to transcript. Eur. J. Biochem. 270. 3280-3288.
- Chung, J.S., Webster, S.G., 2005. Dynamics of in vivo release of molt-inhibiting hormone and crustacean hyperglycemic hormone in the shore crab, Carcinus maenas. Endocrinology 146, 5545-5551.
- Colombani, J., Andersen, D.S., Leopold, P., 2012. Secreted peptide Dilp8 coordinates Drosophila tissue growth with developmental timing. Science 336, 582-585. https:// doi.org/10.1126/science.1216689.
- Covi, J., Gomez, A., Chang, S., Lee, K., Chang, E., Mykles, D., 2008a. Repression of Yorgan ecdysteroidogenesis by cyclic nucleotides and agonists of NO-sensitive guanylyl cyclase. In: Morris, S., Vosloo, A., (Eds.), 4th Meeting of Comparative Physiologists & Biochemists in Africa - Mara 2008 - "Molecules to Migration: The Pressures of Life", Monduzzi Editore International, Bologna, Italy, pp. 37-46.
- Covi, J.A., Bader, B.D., Chang, E.S., Mykles, D.L., 2010. Molt cycle regulation of protein synthesis in skeletal muscle of the blackback land crab, Gecarcinus lateralis, and the differential expression of a myostatin-like factor during atrophy induced by molting or unweighting. J. Exp. Biol. 213, 172–183. https://doi.org/10.1242/jeb.034389.
- Covi, J.A., Chang, E.S., Mykles, D.L., 2009. Conserved role of cyclic nucleotides in the regulation of ecdysteroidogenesis by the crustacean molting gland. Comp. Biochem. Physiol. 152A, 470-477. https://doi.org/10.1016/j.cbpa.2008.12.005
- Covi, J.A., Chang, E.S., Mykles, D.L., 2012. Neuropeptide signaling mechanisms in crustacean and insect molting glands. Invert. Reprod. Devel. 56, 33-49. https://doi. org/10.1080/07924259.2011.588009.
- Covi, J.A., Kim, H.W., Mykles, D.L., 2008b. Expression of alternatively spliced transcripts for a myostatin-like protein in the blackback land crab. Gecarcinus lateralis. Comp. Biochem. Physiol. 150A, 423-430. https://doi.org/10.1016/j.cbpa.2008.04.608.
- Das, S., Mykles, D.L., 2016. A comparison of resources for the annotation of a de novo assembled transcriptome in the molting gland (Y-organ) of the blackback land crab, Gecarcinus lateralis. Integr. Comp. Biol. 56, 1103-1112.
- Das, S., Pitts, N.L., Mudron, M.R., Durica, D.S., Mykles, D.L., 2016. Transcriptome analysis of the molting gland (Y-organ) from the blackback land crab, *Gecarcinus lateralis*. Comp. Biochem. Physiol. 17D, 26–40. https://doi.org/10.1016/j.cbd.2015.11.003.
- Das, S., Vraspir, L., Zhou, W., Durica, D.S., Mykles, D.L., 2018. Transcriptomic analysis of differentially expressed genes in the molting gland (Y-organ) of the blackback land crab, Gecarcinus lateralis, during molt-cycle stage transitions. Comp. Biochem.
- Physiol. 28D, 37–53. https://doi.org/10.1016/j.chd.2018.06.001.

 Dauphin-Villemant, C., Böcking, D., Sedlmeier, D., 1995. Regulation of steroidogenesis in crayfish molting glands: Involvement of protein synthesis. Molec. Cell. Endocrinol. 109, 97-103,
- De Santis, C., Wade, N.M., Jerry, D.R., Preston, N.P., Glencross, B.D., Sellars, M.J., 2011. Growing backwards: an inverted role for the shrimp ortholog of vertebrate myostatin and GDF11. J. Exp. Biol. 214, 2671-2677. https://doi.org/10.1242/jeb.056374.
- Dell, S., Sedlmeier, D., Böcking, D., Dauphin-Villemant, C., 1999. Ecdysteroid biosynthesis in crayfish Y-organs: Feedback regulation by circulating ecdysteroids. Arch. Insect Biochem. Physiol. 41, 148-155.
- Derynck, R., Budi, E.H., 2019. Specificity, versatility, and control of TGF-beta family signaling. Sci. Signaling 12, eaav5183. https://doi.org/10.1126/scisignal.aav5183.
- Devi, A.R.S., Smija, M.K., Sagar, B.K.C., 2015. Light and electron microscopic studies on the Y organ of the freshwater crab Travancoriana schirnerae. J. Microsc. Ultrastruct. 3,
- Drach, P., 1939. Meu et cycle d'intermue chez les Crustaces Decapodes. Ann. Inst. Oceanogr. Monaco. 19, 103–391. Drach, P., Tchernigovtzeff, C., 1967. Sur la méthode de détermination des stades d'in-
- termue et son application générale aux Crustacés. Vie Et Milieu Serie a-Biologie Marine 18, 595-609.
- Duan, Y.H., Li, F.N., Tan, K.R., Liu, H.N., Li, Y.H., Liu, Y.Y., et al., 2015. Key mediators of intracellular amino acids signaling to mTORC1 activation. Amino Acids 47, 857-867. https://doi.org/10.1007/s00726-015-1937-x
- Francis, S.H., Blount, M.A., Corbin, J.D., 2011, Mammalian cyclic nucleotide phosphodiesterases: Molecular mechanisms and physiological functions. Physiol. Rev. 91, 651-690. https://doi.org/10.1152/physrev.00030.2010.
- Garelli, A., Gontijo, A.M., Miguela, V., Caparros, E., Dominguez, M., 2012. Imaginal discs secrete insulin-like peptide 8 to mediate plasticity of growth and maturation. Science 336, 579-582. https:/ //doi.org/10.1126/science.1216735
- Ghimire, K., Altmann, H.M., Straub, A.C., Isenberg, J.S., 2017. Nitric oxide: what's new to NO? Am. J. Physiol. 312, C254–C262. https://doi.org/10.1152/ajpcell.00315.2016. Gontijo, A.M., Garelli, A., 2018. The biology and evolution of the Dilp8-Lgr3 pathway: A
- relaxin-like pathway coupling tissue growth and developmental timing control. Mech. Development 154, 44-50. https://doi.org/10.1016/j.mod.2018.04.005
- Groenewoud, M.J., Zwartkruis, F.J.T., 2013. Rheb and Rags come together at the lysosome to activate mTORC1. Biochem. Soc. Trans. 41, 951-955. https://doi.org/10. 1042/bst20130037.
- Hamer, M.S., 2015. The proteomic response of the Carcinus maenas Y-organ over the course of the molt cycle. San Luis Obispo. California Polytechnic University, San Luis Obispo, CA USA, pp. 1–113. https://doi.org/10.15368/theses.2015.6.
- Han, D.W., Patel, N., Watson, R.D., 2006. Regulation of protein synthesis in Y-organs of the blue crab (Callinectes sapidus): Involvement of cyclic AMP. J. Exp. Zool. 305A,
- Han, D.W., Watson, R.D., 2005. Trimeric G proteins in crustacean (Callinectes sapidus) Yorgans: Occurrence and functional link to protein synthesis. J. Exp. Zool. 303A 441-447
- Hausch, F., Kozany, C., Theodoropoulou, M., Fabian, A.K., 2013. FKBPs and the Akt/ mTOR pathway. Cell Cycle. 12, 2366–2370. https://doi.org/10.4161/cc.25508
- Head, T.B., Mykles, D.L., Tomanek, L., 2019. Proteomic analysis of the crustacean molting gland (Y-organ) over the course of the molt cycle. Comp. Biochem. Physiol. 29D, 193-210. https://doi.org/10.1016/j.cbd.2018.11.011.
- Holland, C.A., Skinner, D.M., 1976. Interactions between molting and regeneration in the land crab. Biol. Bull. 150, 222-240.

- Hopkins, P.M., 2012. The eyes have it: A brief history of crustacean neuroendocrinology. Gen. Comp. Endocrinol. 175, 357-366.
- Hopkins, P.M., Das, S., 2015. Regeneration in crustaceans. In: Chang, E.S., Thiel, M. (Eds.), The Natural History of the Crustacea, vol. 4: Physiology. Oxford University Press, Oxford, U.K., pp. 168-198.
- Hrycay, E.G., Bandiera, S.M., 2015. Monooxygenase, peroxidase and peroxygenase properties and reaction mechanisms of cytochrome P450 enzymes. In: Hrycay, E.G., Bandiera, S.M., (Eds.), Monooxygenase, Peroxidase and Peroxygenase Properties and Mechanisms of Cytochrome P450, pp. 1-61.
- Inman, G.J., Nicolas, F.J., Callahan, J.F., Harling, J.D., Gaster, L.M., Reith, A.D., et al., 2002. SB-431542 is a potent and specific inhibitor of transforming growth factor-beta superfamily type I activin receptor-like kinase (ALK) receptors ALK4, ALK5, and ALK7. Molec. Pharmacol. 62, 65-74.
- Jaszczak, J.S., Wolpe, J.B., Bhandari, R., Jaszczak, R.G., Halme, A., 2016. Growth coordination during Drosophila melanogaster imaginal disc regeneration is mediated by signaling through the relaxin receptor Lgr3 in the prothoracic gland. Genetics 204,
- 703–709. https://doi.org/10.1534/genetics.116.193706.

 Jaszczak, J.S., Wolpe, J.B., Dao, A.Q., Halme, A., 2015. Nitric oxide synthase regulates growth coordination during *Drosophila melanogaster* imaginal disc regeneration. Genetics 200, 1219–1228. https://doi.org/10.1534/genetics.115.178053.
- Jung, H., Lyons, R.E., Hurwood, D.A., Mather, P.B., 2013. Genes and growth performance in crustacean species: a review of relevant genomic studies in crustaceans and other taxa. Rev. Aquacult. 5, 77-110. https://doi.org/10.1111/raq.12005.
- Kang, B.K., Spaziani, E., 1995. Uptake of high-density lipoprotein by Y-organs of the crab g, B.K., Spazialii, E., 1753. Optake of inginiteristy in proposed by a solution of the absence of lysosomal processing. J. Exp. Zool. 273, 425–433.
- Katayama, H., Nagata, K., Ohira, T., Yumoto, F., Tanokura, M., Nagasawa, H., 2003. The solution structure of molt-inhibiting hormone from the kuruma prawn Marsupenaeus japonicus. J. Biol. Chem. 278, 9620-9623.
- Kim, H.W., Batista, L.A., Hoppes, J.L., Lee, K.J., Mykles, D.L., 2004a. A crustacean nitric oxide synthase expressed in nerve ganglia, Y-organ, gill and gonad of the tropical land crab, *Gecarcinus lateralis*. J. Exp. Biol. 207, 2845–2857.

 Kim, H.W., Mykles, D.L., Goetz, F.W., Roberts, S.B., 2004b. Characterization of a myos-
- tatin-like gene from the bay scallop, Argopecten irradians. Biochim. Biophys. Acta. 1679, 174–179.
- Kim, J., Guan, K.L., 2019. mTOR as a central hub of nutrient signalling and cell growth. Nature Cell Biol. 21, 63-71. https://doi.org/10.1038/s41556-018-0205-1.
- Kim, K.S., Jeon, J.-M., Kim, H.W., 2009. A myostatin-like gene expressed highly in the
- muscle tissue of Chinese mitten crab, *Eriocheir sinensis*. Fish. Aqua. Sci. 12, 185–193. Kim, K.S., Kim, Y.J., Jeon, J.M., Kang, Y.S., Oh, C.W., Kim, H.W., 2010. Molecular characterization of myostatin-like genes expressed highly in the muscle tissue from Morotoge shrimp Pandalopsis japonica. Aquaculture Res. 41, e862-e871. https://doi. org/10.1111/j.1365-2109.2010.02610.x.
- Kim, Y.J., Spalovska-Valachova, I., Cho, K.H., Zitnanova, I., Park, Y., Adams, M.E., et al., 2004c. Corazonin receptor signaling in ecdysis initiation. Proc. Natl. Acad. Sci. USA 101, 6704–6709. https://doi.org/10.1073/pnas.0305291101.
- Lachaise, A., Le Roux, A., Hubert, M., Lafont, R., 1993. The molting gland of crustaceans: localization, activity, and endocrine control (a review). J. Crustacean Biol. 13, 198-234.
- Lachaise, F., Somme, G., Carpentier, G., Granjeon, E., Webster, S., Baghdassarian, D., 1996. A transaldolase - An enzyme implicated in crab steroidogenesis. Endocrine 5,
- Layalle, S., Arquier, N., Leopold, P., 2008. The TOR pathway couples nutrition and developmental timing in *Drosophila*. Dev. Cell 15, 568-577. https://doi.org/10.1016/j. devcel.2008.08.003.
- Lee, J.H., Momani, J., Kim, Y.M., Kang, C.K., Choi, J.H., Baek, H.J., et al., 2015. Effective RNA-silencing strategy of Lv-MSTN/GDF11 gene and its effects on the growth in shrimp, Litopenaeus vannamei. Comp. Biochem. Physiol. 179B, 9-16. https://doi.org/ 10.1016/j.cbpb.2014.09.005
- Lee, S.G., Bader, B.D., Chang, E.S., Mykles, D.L., 2007a. Effects of elevated ecdysteroid on tissue expression of three guanylyl cyclases in the tropical land crab Gecarcinus lateralis: possible roles of neuropeptide signaling in the molting gland. J. Exp. Biol. 210, 3245-3254.
- Lee, S.G., Kim, H.W., Mykles, D.L., 2007b. Guanylyl cyclases in the tropical land crab, Gecarcinus lateralis: Cloning of soluble (NO-sensitive and -insensitive) and membrane receptor forms. Comp. Biochem. Physiol. 2D, 332-344.
- Lee, S.G., Mykles, D.L., 2006. Proteomics and signal transduction in the crustacean molting gland. Integr. Comp. Biol. 46, 965–977. Liu, G.Y., Sabatini, D.M., 2019. mTOR at the nexus of nutrition, growth, ageing and
- disease. Nature Rev. Molec. Cell Biol. 29. https://doi.org/10.1038/s41580-019-
- Luo, K., 2017. Signaling cross talk between TGF-beta/Smad and other signaling pathways. Cold Spring Harbor Perspect. Biol. 9 pii, a022137. https://doi.org/10.1101/
- Lv, J.J., Liu, P., Gao, B.Q., Wang, Y., Wang, Z., Chen, P., et al., 2014. Transcriptome analysis of the Portunus trituberculatus: de novo assembly, growth-related gene identification and marker discovery. PLoS One 9, e94055. https://doi.org/10.1371/ journal.pone.0094055.
- Macias, M.J., Martin-Malpartida, P., Massague, J., 2015. Structural determinants of Smad function in TGF-beta signaling. Trends Biochem. Sci. 40, 296-308. https://doi.org/ 10.1016/j.tibs.2015.03.012.
- MacLea, K.S., Abuhagr, A.M., Pitts, N.L., Covi, J.A., Bader, B.D., Chang, E.S., et al., 2012. Rheb, an activator of target of rapamycin, in the blackback land crab, Gecarcinus lateralis: cloning and effects of molting and unweighting on expression in skeletal muscle. J. Exp. Biol. 215, 590-604. https://doi.org/10.1242/jeb.062869.
- MacLea, K.S., Covi, J.A., Kim, H.W., Chao, E., Medler, S., Chang, E.S., et al., 2010. Myostatin from the American lobster, Homarus americanus: Cloning and effects of molting on expression in skeletal muscles. Comp. Biochem. Physiol. 157A, 328-337. https://doi.org/10.1016/J.cbpa.2010.07.024.
- Marchal, E., Vandersmissen, H.P., Badisco, L., Van de Velde, S., Verlinden, H., Iga, M.,

- et al., 2010. Control of ecdysteroidogenesis in prothoracic glands of insects: A review. Peptides 31, 506-519. https://doi.org/10.1016/j.peptides.2009.08.020.
- Mattson, M.P., 1986. New insights into neuroendocrine regulation of the crustacean molt cycle, Zool, Sci. 3, 733-744.
- Mattson, M.P., Spaziani, E., 1986a. Regulation of crab Y-organ steroidogenesis in vitro -Evidence that ecdysteroid production increases through activation of cAMP-phosphodiesterase by calcium-calmodulin. Molec. Cell. Endocrinol. 48, 135-151.
- Mattson, M.P., Spaziani, E., 1986b. Regulation of Y-organ ecdysteroidogenesis by moltinhibiting hormone in crabs: involvement of cyclic AMP-mediated protein synthesis. Gen. Comp. Endocrinol. 63, 414-423.
- Mattson, M.P., Spaziani, E., 1987. Demonstration of protein kinase C activity in crustacean Y-organs and partial definition of its role in regulation of ecdysteroidogenesis. Molec. Cell. Endocrinol. 49, 159-171.
- McCarthy, J.F., Skinner, D.M., 1977. Proecdysial changes in serum ecdysone titers, gastrolith formation, and limb regeneration following molt induction by limb autotomy and/or eyestalk removal in land crab, Gecarcinus lateralis. Gen. Comp. Endocrinol. 33, 278_202
- McDonald, A.A., Chang, E.S., Mykles, D.L., 2011. Cloning of a nitric oxide synthase from green shore crab. Carcinus maenas: A comparative study of the effects of evestalk ablation on expression in the molting glands (Y-organs) of C. maenas, and blackback land crab Gecarcinus lateralis. Comp. Biochem. Physiol. 158A, 150-162. https://doi. org/10.1016/j.cbpa.2010.10.013.
- Mykles, D.L., 1980. The mechanism of fluid absorption at ecdysis in the American lobster, Homarus americanus. J. Exp. Biol. 84, 89-101.
- Mykles, D.L., 2001. Interactions between limb regeneration and molting in decapod crustaceans. Am. Zool. 41, 399–406.
- Mykles, D.L., 2011. Ecdysteroid metabolism in crustaceans. J. Steroid Biochem. Molec. Biol. 127, 196-203. https://doi.org/10.1016/j.jsbmb.2010.09.001
- Mykles, D.L., Adams, M.E., Gade, G., Lange, A.B., Marco, H.G., Orchard, I., 2010a. Neuropeptide action in insects and crustaceans. Physiol. Biochem. Zool. 83, 836-846. https://doi.org/10.1086/648470.
- Mykles, D.L., Burnett, K.G., Durica, D.S., Joyce, B.L., McCarthy, F.M., Schmidt, C.J., et al., 2016. Resources and recommendations for using transcriptomics to address grand challenges in comparative biology. Integr. Comp. Biol. 56, 1183–1191.
- Mykles, D.L., Ghalambor, C.K., Stillman, J.H., Tomanek, L., 2010b. Grand challenges in comparative physiology: Integration across disciplines and across levels of biological organization. Integr. Comp. Biol. 50, 6-16. https://doi.org/10.1093/icb/icq015
- Mykles, D.L., Hui, J.H.L., 2015. Neocaridina denticulata: A decapod crustacean model for functional genomics. Integr. Comp. Biol. 55, 891-897. https://doi.org/10.1093/icb/ icv050
- Mykles, D.L., Medler, S., 2015. In: Chang, E.S., Thiel, M. (Eds.), The Natural History of the Crustacea 4. Physiology, Oxford University Press, Oxford, U.K, pp. 134–167.
- Nakatsuji, T., Lee, C.Y., Watson, R.D., 2009. Crustacean molt-inhibiting hormone: Structure, function, and cellular mode of action. Comp. Biochem. Physiol. 152A, 139-148. https://doi.org/10.1016/j.cbpa.2008.10.012
- Nakatsuji, T., Sonobe, H., 2003. Measurement of molt-inhibiting hormone titer in hemolymph of the American crayfish, *Procambarus clarkii*, by time-resolved fluoroimmunoassay. Zool. Sci. 20, 999–1001.
- Nakatsuji, T., Sonobe, H., 2004. Regulation of ecdysteroid secretion from the Y-organ by molt-inhibiting hormone in the American crayfish, Procambarus clarkii. Gen. Comp. Endocrinol. 135, 358-364.
- Nakatsuji, T., Sonobe, H., Watson, R.D., 2006. Molt-inhibiting hormone-mediated regulation of ecdysteroid synthesis in Y-organs of the crayfish (Procambarus clarkii): involvement of cyclic GMP and cycle nucleotide phosphodiesterase. Molec. Cell. Endocrinol. 253, 76-82.
- Nickel, J., ten Dijke, P., Mueller, T.D., 2018. TGF-beta family co-receptor function and signaling. Acta Biochim. Biophys. Sinica 50, 12-36. https://doi.org/10.1093/abbs/
- Niwa, R., Niwa, Y.S., 2014. Enzymes for ecdysteroid biosynthesis: their biological functions in insects and beyond. Biosci. Biotechnol. Biochem. 78, 1283-1292. https://doi. org/10 1080/09168451 2014 942250
- Nong, W.Y., Chai, Z.Y.H., Jiang, X.S., Qin, J., Ma, K.Y., Chan, K.M., et al., 2020. A crustacean annotated transcriptome (CAT) database. BMC Genomics 21. https://doi. org/10.1186/s12864-019-6433-3.
- Oliphant, A., Alexander, J.L., Swain, M.T., Webster, S.G., Wilcockson, D.C., 2018. Transcriptomic analysis of crustacean neuropeptide signaling during the moult cycle in the green shore crab, Carcinus maenas. BMC Genomics 19, 711. https://doi.org/10. 1186/s12864-018-5057-3
- Peng, T., Gong, J., Jin, Y.Z., Zhou, Y.P., Tong, R.S., Wei, X., et al., 2018. Inhibitors of phosphodiesterase as cancer therapeutics. Eur. J. Med. Chem. 150, 742–756. https:// doi.org/10.1016/j.ejmech.2018.03.046.
- Pitts, N.L., Mykles, D.L., 2017. Localization and expression of molt-inhibiting hormone and nitric oxide synthase in the central nervous system of the green shore crab, Carcinus maenas, and the blackback land crab, Gecarcinus lateralis. Comp. Biochem. Physiol. 203A, 328–340. https://doi.org/10.1016/j.cbpa.2016.10.012. Pitts, N.L., Schulz, H.M., Oatman, S.R., Mykles, D.L., 2017. Elevated expression of neu-
- ropeptide signaling genes in the eyestalk ganglia and Y-organ of Gecarcinus lateralis individuals that are refractory to molt induction. Comp. Biochem. Physiol. 214B, 66–78. https://doi.org/10.1016/j.cbpa.2017.09.011.
- Qian, Z.Y., Mi, X., Wang, X.Z., He, S.L., Liu, Y.J., Hou, F.J., et al., 2013. cDNA cloning and expression analysis of myostatin/GDF11 in shrimp, Litopenaeus vannamei. Comp. Biochem. Physiol. 165A, 30–39. https://doi.org/10.1016/j.cbpa.2013.02.001. Qu, Z., Bendena, W.G., Tobe, S.S., Hui, J.H.L., 2018. Juvenile hormone and sesqui-
- terpenoids in arthropods: Biosynthesis, signaling, and role of microRNA. J. Steroid Biochem. Molec. Biol. 184, 69–76. https://doi.org/10.1016/j.jsbmb.2018.01.013.
- Reamur, M., 1718a. Aux observations sur la mue des ecrevisses, donnee dans les memoires de 1712. Histoire de l'Academie Royale des Sciences 1718: 263-274.
- Reamur, M., 1718b. Sur la mue des ecrevisses. Histoire de l'Academie Royale des Sciences 1718: 22-24.
- Rewitz, K.F., Yamanaka, N., O'Connor, M.B., 2013. Developmental checkpoints and

- feedback circuits time insect maturation. In: Shi, Y.B. (Ed.), Animal Metamorphosis,
- Rifai, N.M., Mykles, D.L., 2019. Effects of molt induction methods on cyclic nucleotide phosphodiesterase expression in the decapod crustacean molting gland. Integr. Comp. Biol. 59, E194.
- Rodenfels, J., Lavrynenko, O., Ayciriex, S., Sampaio, J.L., Carvalho, M., Shevchenko, A., et al., 2014. Production of systemically circulating hedgehog by the intestine couples nutrition to growth and development. Genes Devel. 28, 2636-2651. https://doi.org/ 10.1101/gad.249763.114.
- Roegner, M.E., Chen, H.Y., Watson, R.D., 2018. Molecular cloning and characterization of a sarco/endoplasmic reticulum Ca²⁺ ATPase (SERCA) from Y-organs of the blue crab (*Callinectes sapidus*). Gene 673, 12–21. https://doi.org/10.1016/j.gene.2018.06.018.
- Roegner, M.E., Roer, R.D., Watson, R.D., 2019. Sarco/endoplasmic reticulum Ca²⁺ ATPase (SERCA) transcript abundance in Y-organs and ecdysteroid titer in hemolymph during a molting cycle of the blue crab, Callinectes sapidus. Comp. Biochem. Physiol. 229A, 76-80. https://doi.org/10.1016/j.cbpa.2018.12.006.
- Romero-Pozuelo, J., Demetriades, C., Schroeder, P., Teleman, A.A., 2017. CycD/Cdk4 and discontinuities in Dpp signaling activate TORC1 in the Drosophila wing disc. Dev. Cell. 42, 376–387. https://doi.org/10.1016/j.devcel.2017.07.019.
- Sagi, A., Manor, R., Ventura, T., 2013. Gene silencing in crustaceans: From basic research to biotechnologies. Genes 4, 620-645. https://doi.org/10.3390/genes4040620.
- Saïdi, B., De Bessé, N., Webster, S.G., Sedlmeier, D., Lachaise, F., 1994. Involvement of cAMP and cGMP in the mode of action of molt-inhibiting hormone (MIH) a neuropeptide which inhibits steroidogenesis in a crab. Molec. Cell. Endocrinol. 102, 53–61. Salminen, A., Kaarniranta, K., Kauppinen, A., 2016. AMPK and HIF signaling pathways
- regulate both longevity and cancer growth: the good news and the bad news about survival mechanisms. Biogerontol. 17, 655-680. https://doi.org/10.1007/s10522-
- Sarasvathi, P.E., Bhassu, S., Maningas, M.B.B., Othman, R.Y., 2015. Myostatin: A potential growth-regulating gene in giant river prawn Macrobrachium rosenbergii. J. World Aquaculture Soc. 46, 624-634. https://doi.org/10.1111/jwas.12238.
- Saxton, R.A., Sabatini, D.M., 2017. mTOR signaling in growth, metabolism, and disease. Cell 168, 960–976. https://doi.org/10.1016/j.cell.2017.02.004.
 Sedlmeier, D., Fenrich, R., 1993. Regulation of ecdysteroid biosynthesis in crayfish Y-
- organs: I. Role of cyclic nucleotides. J. Exp. Zool. 265, 448–453.
- Sedlmeier, D., Seinsche, A., 1998. Ecdysteroid synthesis in the crustacean Y-organ: role of cyclic nucleotides and Ca²⁺. Soc. Exp. Biol. 65, 125–137.
- Shen, W.Y., Ren, G., Zhu, Y.R., Zhang, X.D., 2015. Characterization of MSTN/GDF11 gene from shrimp Macrobrachium nipponense and its expression profiles during molt cycle and after evestalk ablation, Genes & Genomics 37, 441–449, https://doi.org/10 1007/s13258-015-0273-6.
- Shi, L., Wu, Y., Sheen, J., 2018. TOR signaling in plants: conservation and innovation. Development 145, dev160887. https://doi.org/10.1242/dev.160887
- Shimobayashi, M., Hall, M.N., 2014. Making new contacts: the mTOR network in metabolism and signalling crosstalk. Nature Rev. Molec. Cell Biol. 15, 155-162. https:// doi.org/10.1038/nrm3757.
- Shyamal, S., Das, S., Guruacharya, A., Mykles, D.L., Durica, D.S., 2018. Transcriptomic analysis of crustacean molting gland (Y-organ) regulation via the mTOR signaling pathway. Sci. Rep. 8, 7307. https://doi.org/10.1038/s41598-018-25368-x.
- Shyamal, S., Sudha, K., Gayathri, N., Anilkumar, G., 2014. The Y-organ secretory activity fluctuates in relation to seasons of molt and reproduction in the brachyuran crab, Metopograpsus messor (Grapsidae): Ultrastructural and immunohistochemical study. Gen. Comp. Endocrinol. 196, 81-90.
- Sin, Y.W., Kenny, N.J., Qu, Z., Chan, K.W., Chan, K.W.S., Cheong, S.P.S., et al., 2014. Identification of putative ecdysteroid and juvenile hormone pathway genes in the shrimp *Neocaridina denticulata*. Gen. Comp. Endocrinol. 214, 167–176.
- Skinner, D.M., 1962. The structure and metabolism of a crustacean integumentary tissue during a molt cycle. Biol. Bull. 123, 635-647.
- Skinner, D.M., 1985. In: Bliss, D.E., Mantel, L.H. (Eds.), The Biology of Crustacea 9. Academic Press, New York, pp. 43–146. Skinner, D.M., Graham, D.E., 1970. Molting in land crabs: stimulation by leg removal.
- Science 169, 383-385. Skinner, D.M., Graham, D.E., 1972. Loss of limbs as a stimulus to ecdysis in Brachyura
- (true crabs). Biol. Bull. 143, 222–233.
- Smija, M.K., Sudha, D.A.R., 2016. Histological changes of Y organ in Travancoriana schirnerae during moult cycle and in de-eyestalked crabs. Turkish J. Fish. Aquatic Sci. 16, 533-544. https://doi.org/10.4194/1303-2712-v16_3_06.
- Smith, R.I., 1940. Studies on the effects of eyestalk removal upon young crayfish (Cambarus clarkii Girard), Biol. Bull. 79, 145-152.
- Snyder, M.J., Chang, E.S., 1991. Ecdysteroids in relation to the molt cycle of the American lobster, Homarus americanus. I. Hemolymph titers and metabolites. Gen. Comp. Endocrinol. 81, 133-145.
- Spaziani, E., Jegla, T.C., Wang, W.L., Booth, J.A., Connolly, S.M., Conrad, C.C., et al., 2001. Further studies on signaling pathways for ecdysteroidogenesis in crustacean Yorgans. Am. Zool. 41, 418-429.
- Spaziani, E., Mattson, M.P., Wang, W.N.L., McDougall, H.E., 1999. Signaling pathways for ecdysteroid hormone synthesis in crustacean Y-organs. Am. Zool. 39, 496-512.
- Spindler, K.D., Adelung, D., Tchernigovtzeff, C., 1974. A comparison of the methods of molt staging according to Drach and to Adelung in the common shore crab Carcinus maenas. Z. Naturforsch. C 29, 754-756.
- Stewart, M.J., Stewart, P., Sroyraya, M., Soonklang, N., Cummins, S.F., Hanna, P.J., et al., 2013. Cloning of the crustacean hyperglycemic hormone and evidence for molt-inhibiting hormone within the central nervous system of the blue crab Portunus

- pelagicus. Comp. Biochem. Physiol. 164A, 276-290. https://doi.org/10.1016/j.cbpa. 2012.10.029
- Swall, M.E., Benrabaa, S.A., Mykles, D.L., 2019, Characterization of Shed genes in the molting gland (Y-organ) of the land crab Gecarcinus lateralis. Integr. Comp. Biol. 59,
- Taylor, J.R.A., Kier, W.M., 2003. Switching skeletons: Hydrostatic support in molting crabs. Science. 301, 209-210.
- Taylor, J.R.A., Kier, W.M., 2006. A pneumo-hydrostatic skeleton in land crabs A sophisticated dual support system enables a crab to stay mobile immediately after moulting. Nature 440, 1005.
- Teleman, A.A., 2010. Molecular mechanisms of metabolic regulation by insulin in Drosophila, Biochem, J. 425, 13–26, https://doi.org/10.1042/bi20091181.
- Tom, M., Manfrin, C., Giulianini, P.G., Pallavicini, A., 2013. Crustacean oxi-reductases protein sequences derived from a functional genomic project potentially involved in ecdysteroid hormones metabolism - A starting point for function examination. Gen.
- Comp. Endocrinol. 194, 71–80. https://doi.org/10.1016/j.ygcen.2013.09.003.

 Tran, N.M., Mykles, D.L., Elizur, A., Ventura, T., 2019. Characterization of G-protein coupled receptors from the blackback land crab *Gecarcinus lateralis* Y organ transcriptome over the molt cycle. BMC Genomics 20, 74. https://doi.org/10.1186/ s12864-018-5363-9
- Van Hiel, M.B., Vandersmissen, H.P., Van Loy, T., Broeck, J.V., 2012. An evolutionary comparison of leucine-rich repeat containing G protein-coupled receptors reveals a novel LGR subtype. Peptides 34, 193-200. https://doi.org/10.1016/j.peptides.2011. 11.004.
- Veenstra, J.A., 2015. The power of next-generation sequencing as illustrated by the neuropeptidome of the crayfish *Procambarus clarkii*. Gen. Comp. Endocrinol. 224,
- Ventura, T., Bose, U., Fitzgibbon, Q.P., Smith, G.G., Shaw, P.N., Cummins, S.F., et al., 2017. CYP450s analysis across spiny lobster metamorphosis identifies a long sought missing link in crustacean development. J. Steroid Biochem. Molec. Biol. 171, 262-269. https://doi.org/10.1016/j.jsbmb.2017.04.007.
- Ventura, T., Cummins, S.F., Fitzgibbon, Q., Battaglene, S., Elizur, A., 2014. Analysis of the central nervous system transcriptome of the eastern rock lobster Sagmariasus ver reauxi reveals its putative neuropeptidome. PLoS One 9, e97323. https://doi.org/10. 1371/journal.pone.0097323.
- Ventura, T., Palero, F., Rotllant, G., Fitzgibbon, Q.P., 2018. Crustacean metamorphosis: an omics perspective. Hydrobiologia 825, 47-60. https://doi.org/10.1007/s10750-017-3445
- Webster, S.G., 1993. High-affinity binding of putative moult-inhibiting hormone (MIH) and crustacean hyperglycaemic hormone (CHH) to membrane-bound receptors on the Y-organ of the shore crab Carcinus maenas, Proc. R. Soc. Lond. [Biol.] 251, 53-59.
- Webster, S.G., 2015. Endocrinology of metabolism and water balance: Crustacean hyperglycemic hormone. In: Chang, E.S., Thiel, M. (Eds.), The Natural History of the Crustacea, vol. 4: Physiology. Oxford Press, Oxford, pp. 36–67.
- Webster, S.G., 2015. Endocrinology of molting. In: Chang, E.S., Thiel, M. (Eds.), The Natural History of the Crustacea, vol. 4: Physiology. Oxford Press, Oxford, pp. 1–35.
- Webster, S.G., Keller, R., Dircksen, H., 2012. The CHH-superfamily of multifunctional peptide hormones controlling crustacean metabolism, osmoregulation, moulting, and reproduction. Gen. Comp. Endocrinol. 175, 217–233. https://doi.org/10.1016/j.
- Weichhart, T., 2018. mTOR as regulator of lifespan, aging, and cellular senescence: A mini-review. Gerontology 64, 127-134. https://doi.org/10.1159/000484629
- Wittmann, A.C., Benrabaa, S.A.M., López-Cerón, D.A., Chang, E.S., Mykles, D.L., 2018. Effects of temperature on survival, moulting, and expression of neuropeptide and mTOR signalling genes in juvenile Dungeness crab (Metacarcinus magister). J. Exp. Biol. 221, jeb187492. https://doi.org/10.1242/jeb.187492.
- Wu, N., Yang, M.Y., Gaur, U., Xu, H.L., Yao, Y.F., Li, D.Y., 2016. Alpha-ketoglutarate: Physiological functions and applications. Biomol. Therapeutics 24, 1-8. https://doi. org/10.4062/biomolther.2015.078.
- Yamanaka, N., Rewitz, K.F., O'Connor, M.B., 2013. Ecdysone control of developmental transitions: Lessons from Drosophila research. Berenbaum, M.R. (Ed.), Ann. Rev. Entomol. 58, 497-516.
- Yang, Q., Inoki, K., Kim, E., Guan, K.L., 2006. TSC1/TSC2 and Rheb have different effects on TORC1 and TORC2 activity. Proc. Natl. Acad. Sci. USA 103, 6811-6816. https:/ doi.org/10.1073/pnas.0602282103.
- Yu, X.L., Chang, E.S., Mykles, D.L., 2002. Characterization of limb autotomy factorproecdysis (LAF $_{\mathrm{pro}}$), isolated from limb regenerates, that suspends molting in the land crab Gecarcinus lateralis. Biol. Bull. 202, 204-212.
- Zeleny, C., 1905. Compensatory regulation. J. Exp. Zool. 2, 347–369. Zhang, B.L., Wang, L.J., Sun, L., Zhang, H.L., Wu, X.M., Sun, Y., et al., 2014. Identifying significant crosstalk of pathways in tuberous sclerosis complex. Eur. Rev. Med. Pharmacol. Sci. 18, 2482-2490.
- Zhang, X.J., Yuan, J.B., Sun, Y.M., Li, S.H., Gao, Y., Yu, Y., et al., 2019. Penaeid shrimp genome provides insights into benthic adaptation and frequent molting. Nature Commun. 10. https://doi.org/10.1038/s41467-018-08197-4.
- Zhou, Y.L., Li, B., Xu, Y.P., Wang, L.Z., Gu, W.B., Liu, Z.P., et al., 2019. The Activin-like ligand Dawdle regulates innate immune responses through modulating NF-kappa B signaling in mud crab Scylla paramamosain. Dev. Comp. Immunol. 101, 103450. https://doi.org/10.1016/j.dci.2019.103450.
- Zhuo, R.Q., Zhou, T.T., Yang, S.P., Chan, S.M.F., 2017. Characterization of a molt-related myostatin gene (FmMstn) from the banana shrimp Fenneropenaeus merguiensis. Gen. Comp. Endocrinol. 248, 55–68. https://doi.org/10.1016/j.ygcen.2017.03.010.